HIV Env trimers elicit NHP apex cross-neutralizing antibodies mimicking human bNAbs

Javier Guenaga[1,*], Monika Adori[2,*], Shridhar Bale[1,*], Swastik Phulera[3,*], Ioannis Zygouras[2], Fabian-Alexander Schleich[2], Xaquin Castro Dopico[2], Sashank Agrawal[3], Miyo Ota[1], Richard Wilson[1], Jocelyn Cluff[1], Tamar Dzvelaia[1], Marco Mandolesi[2], Agnes Walsh[1], Mariane B. Melo[1], Laurent Verkoczy[6], Darrell J. Irvine[1,7], Martin Corcoran[1], Ian A. Wilson[3], Diane Carnathan[5], Guido Silvestri[5] Andrew B. Ward[3], Gabriel Ozorowski[3], Gunilla B. Karlsson Hedestam[2,*,+] and Richard T. Wyatt[1,*,+]

[1] Department of Immunology and Microbiology, The Scripps Research Institute, La Jolla, CA, USA

[2] Department of Microbiology, Tumor and Cell Biology, Karolinska Institutet, SE-171 77 Stockholm, Sweden

[3] Department of Integrative Structural and Computational Biology, The Scripps Research Institute, La Jolla, CA, USA

[4]Vaccine Research Center, National Institute of Allergy and Infectious Diseases, National Institutes of Health, Bethesda, MD, USA

[5]Division of Microbiology and Immunology, Emory National Primate Research Center, Emory University, Atlanta, GA, USA

[6] Applied Biomedical Science Institute, 11011 Via Frontera, San Diego, CA 92127

[7]Howard Hughes Medical Institute, 4000 Jones Bridge Rd., Chevy Chase, MD, 20815, USA

*Contributed equally

Lead contact: Richard T. Wyatt, email – wyatt@scripps.edu

[+] To whom correspondence should be addressed:

Gunilla B. Karlsson Hedestam, email - gunilla.karlsson.hedestam@ki.se;

Richard T. Wyatt, email - wyatt@scripps.edu

Abstract

As a chronically replicating virus, HIV has evolved extreme sequence variability and effective shielding of functionally constrained spike protein determinants by host-derived glycans. Broadly neutralizing antibodies (bNAbs), though rare, can be isolated from people living with HIV, revealing conserved Env sites as key targets for vaccine development. One such target is the apex of the envelope glycoprotein (Env) spike. Here, we identified a vaccination strategy using heterologous HIV Env trimers covalently coupled to liposomes for multivalent display that resulted in the elicitation of cross-neutralizing HIV serum antibody responses in all immunized non-human primates (NHPs). Critically, we isolated a set of monoclonal antibodies (mAbs) that cross-neutralized multiple divergent HIV clinical isolates. High-resolution cryoEM structural analysis of mAbs from three different NHPs demonstrated that they targeted the Env trimer apex in a manner remarkably similar to that of the human infection-elicited, apex-directed bNAb PG9, representing a substantial advance in HIV vaccine development.

Keywords: Vaccination, HIV-1 Env apex-targeting, monoclonal antibodies, cross-neutralization, rhesus macaques.

Introduction

The development of an effective prophylactic HIV vaccine capable of reducing the spread of the virus remains a high priority public health goal. However, chronic HIV replication in infected hosts drives immune evasion, [1-3] making vaccine development extremely challenging. The sole neutralizing determinant on the surface of the virus is the trimeric envelope glycoprotein (Env) spike (Figure 1A), which has evolved to evade host antibody responses by incorporating host-derived N-glycans and altering variable domains during replication.[4,5] Broadly neutralizing antibodies (bNAbs), which arise infrequently in people living with HIV-1 (PLWH), can penetrate and, in some cases, co-recognize components of the glycan shield and underlying protein structures, thereby revealing sites of vulnerability. These include the Env trimer apex (Figure 1A), the primary CD4 receptor binding site, V3 glycan site, and functionally constrained regions of the HIV spike proximal to the viral membrane.[6,7]

Elicitation of apex-targeting bNAbs is of particular interest for vaccine design, as such antibodies often require lower levels of somatic hypermutation (SHM) to gain bNAb activity.[8] Several potent apex-directed bNAbs have been isolated from PLWH.[9-15] Generally, the HIV-induced apex bNAbs display very long heavy chain complementarity-determining region 3 (HCDR3) that are characterized by negatively charged 'tips' that interact with the basic HIV Env variable region 2 (V2) C-strand, such as those found in PG9/16, PGT145, VRC26, and CH01-4.[16-20] The glycan-shrouded apex of the Env spike is recognized by the bNAb HCDR3s that penetrate the glycan shield interacting with both the

surrounding glycans and the semi-conserved basic C-strand of V2.[8,19-22] The maturation of these antibodies is driven by the co-evolution of the virus and antibody interactions that include both glycan and protein contacts.[21,23]

Studies show that infection with chimeric simian-human immunodeficiency viruses (SHIVs) elicit apex-targeting bNAbs in non-human primates (NHPs), such as the RHA1 bNAb, [24] as well as other apex-directed cross-neutralizing monoclonal antibodies (mAbs). [25] These findings validate macaques as a suitable model for evaluation of vaccines aimed to stimulate such responses. [24] The SHIV-induced cross-neutralizing serum activity detected in the RHA1-generating NHP was informative to identify virus trimers capable of eliciting apex-directed antibody responses (i.e., Q23.17, ZM233, potently neutralized). In addition, SHIV-induced broadly neutralizing apex-targeting bNAbs can inform HIV vaccine design. However, B cell activation and general immune stimulus by a replicating virus differ substantially from that induced by recombinant protein subunit vaccines. It is less certain whether subunit vaccination can elicit comparable apex-targeting neutralizing antibody responses in animal models, an important first step towards translatable human vaccine strategies.

Here, we screened a set of native-like HIV Env trimers using the apex-targeting bNAb, RHA1 and its inferred germline (gL) reverted variant (igL RHA1) to identify a potential priming immunogen. For initial priming, we selected Q23.17 HIV strain-derived native flexibly linked (NFL) stabilized trimers based upon their avid binding to the mature RHA1 bNAb and still detectable binding to the igL RHA1 mAb (Figure 1B). [26-28] To enhance B cell priming, we covalently arrayed these trimers on synthetic liposomes [29] and compared the liposome-arrayed platform with soluble NFL trimers in rhesus macaques (Figures 1C and 1D). Following Q23 NFL priming and 'tandem' Env boosting with the heterologous ZM233 NFL trimers, we detected robust serum neutralization of both Q23.17 and ZM233 pseudoviruses in animals from both groups of NHPs. Apex-directed electron microscopy-based polyclonal epitope mapping (EMPEM) densities were detected in all NHPs immunized with the trimer liposomal array. Following sequential boosting with two additional stabilized NFL trimers, we detected tier-2 serum cross-neutralization in all trimer-liposome immunized NHPs. Based on these encouraging results, we isolated a panel of Env-binding mAbs and characterized their genetic, functional and structural properties. CryoEM structures of mAb:trimer complexes at high-resolution showed that mAb apex-targeting mirrors the binding mode of the infection-elicited human bNAb PG9. These findings demonstrate that high-density liposome arrays of germline-guided, native-like Env trimers effectively activate apex-targeting B cells, eliciting antibody responses that recapitulate features described in human infection-driven bNAbs.

Results

102

103 **Identification of stabilized trimers that are well-recognized by an NHP germline-reverted**
104 **apex bNAb**

105

106 Roark et al. (2021) demonstrated that CH505 SHIV infection generated apex-directed polyclonal
107 responses that potently neutralized several apex-sensitive viruses, including Q23.17, ZM233.6, and T-
108 250-4.[24] RHA1, an apex-targeting bNAb was isolated from one of the NHPs in that study. Cross-
109 neutralizing activity in this animal's serum was detected within a year following SHIV infection. Based
110 on these findings, we generated soluble, stabilized, near-native NFL trimers from several of these
111 strains, confirmed their conformational integrity, as described here and previously by bio-layer
112 interferometry (BLI) and differential scanning calorimetry (DSC) (Figures S1A and S1B). [26-28,30] NFL
113 trimers were tested for recognition by the NHP apex-directed RHA1 bNAb and nbNAb PGT145 (Figure
114 S1C). We observed nanomolar binding affinity of mature RHA1 to NFL trimers derived from the Q23
115 and ZM233 HIV-1 strains while only the Q23 NFL trimer displayed micromolar binding affinity to the
116 reverted igL RHA1 antibody (Figure 1B). The germline-reverted RHA1 mAb was designed by reverting
117 both light and heavy chain residues to their inferred naïve sequences, retaining only the mature HCDR3.
118 We next evaluated whether high-avidity, multivalent Q23 NFL trimers arrayed covalently on liposomes
119 (Figure 1C) would enhance binding to igL RHA1 as determined by ELISA. Compared with soluble
120 trimers, liposome-arrayed Q23 NFL trimers, captured by lectin, displayed stronger binding to the igL
121 RHA1 and to the mature PGT145, with comparable 2G12 binding, confirming that equivalent levels of
122 trimers were captured (Figure S1D). To assess B cell activation by the NFL trimer liposomal array, we
123 measured calcium flux in primary murine B cells expressing the unmutated common ancestor (UCA)
124 of the infection-derived, apex-targeting human bNAb, CH01, as well as in the murine K46 cells line
125 expressing the mature bNAb PG16. We detected a substantial increase in intracellular Ca^{2+} flux induced
126 by the multivalent Q23 trimer-liposomes compared to soluble trimers (Figures 1E and S1E), indicating
127 that the multivalent array could potentially activate naïve B cells more effectively.

128

129 **Immunization with Env NFL trimer-liposomes elicits apex-directed, cross-neutralizing**
130 **serum antibodies in all NHPs**

131

132 Twelve NHPs were immunized with Q23 NFL trimers, administered either as soluble trimers (Q1-6) or
133 covalently coupled to high-valency array as trimer-liposomes (Q7-12) (Figure 1D). SMNP was used as
134 the adjuvant throughout the study.[31] To increase engagement of rare apex-bNAb precursors in the NHP
135 repertoire, we opted for a fractionated Q23 NFL priming, dosed over 8 weeks. Antibody responses from
136 serum-purified IgG collected after the Q23 and ZM233 tandem immunization (P2) displayed autologous
137 neutralization of both Q23 and ZM233 pseudovirus in four NHPs from the soluble group and six NHPs

138 from the trimer-liposome group (Figure S1F). The serum-purified IgG was concentrated to a level
139 matching that naturally found in the serum (approximately 10 mg/mL); neutralization is reported as
140 50% inhibitory concentrations (IC_{50}). Eventually all NHPs in both groups developed these responses
141 over subsequent immunizations (P3-P6). Neutralizing serum antibody responses were stronger in the
142 trimer-liposome-immunized NHPs than in the animals inoculated with soluble trimers (Figure S1E). To
143 determine whether the neutralizing antibody responses targeted the HIV Env apex, we used electron
144 microscopy-based polyclonal epitope mapping (EMPEM) to derive images of serum antibodies in
145 complex with the NFL trimer immunogens. EMPEM analysis of the serum IgG-derived Fabs in
146 complex with the Q23 trimer revealed binding densities to the trimer apex in all NHPs from the trimer-
147 liposome group (Figure 1F) and four NHPs from the soluble group (Figure S1G). The NHPs were
148 subsequently immunized every 12 weeks with NFL Env trimers derived from heterologous HIV strains
149 WITO.33, 001428-2.42, RW020.2, and CH119.10. Following immunization with the 001428 NFL
150 trimers (P4), all IgG samples from animals immunized with trimer-liposomes neutralized a sentinel
151 panel of heterologous tier 2 HIV-1 clinical isolates (Figure S1H). The most potent cross-neutralization
152 activity was displayed in the serum IgG derived from NHP Q12. Based on these data, we analyzed the
153 serum by EMPEM to define the predominant cross-binding specificity. We selected three NHPs from
154 the trimer-liposome group (Q8, Q9, and Q12) that displayed neutralization activity against several
155 heterologous HIV strains, including 16055-2.3 and BG505.W6M. Notably, NFLs derived from these
156 strains were not part of the immunization regimen, and we thus analyzed the pooled sera by EMPEM
157 against these heterologous trimers. PolyFab binding densities targeting the Env apex were observed in
158 both 16055 and BG505 trimer-Fab complexes, suggesting that the apex-directed cross-neutralization
159 was likely mediated by the serum IgG corresponding to these EMPEM densities (Figure S1I). The
160 serum IgG from these NHPs also neutralized other apex-sensitive clinical isolates (Figure S1H). From
161 these data, we conclude that our vaccine strategy, prime:boosting with four NFL trimers covalently
162 arrayed on liposomes, elicited apex-directed, cross-neutralizing antibodies in all NHPs. Additional
163 heterologous boosting after the 00148 NFL trimer (by RW020 and CH119 NFLs, P6) generally
164 broadened the cross-neutralizing activity of the serum IgG, particularly for Q2 in the soluble trimer
165 group and for the entire trimer-liposome group (Figure 1G).
166

167 **mAb isolation confirms serum IgG cross-neutralization, demonstrating neutralization**
168 **breadth of clinical isolates**

169 To define the Ab reactivities responsible for the serum IgG cross-neutralization detected in the trimer-
170 liposome-immunized NHPs, we isolated single memory B cells from peripheral blood mononuclear
171 cells (PBMCs) collected at time points P4, P5, and P6, using Q23 and/or BG505 NFL trimers as probes
172 for flow cytometry-based sorting (Figure 2A). We genotyped each NHP for their immunoglobulin (IG)
173 allele repertoire using IgDiscover and assigned all heavy (HC) and light chains (LC) to the closest

174 germline V, D, and J alleles present in that individual animal, enabling precise allele annotation and
175 clarification of clonal relationships.[32-34]Guided by the serum neutralization data, we focused our B cell
176 analysis on NHPs Q9, Q10, and Q12, from which we recovered 103, 159, and 393 paired heavy and
177 light chains, which grouped into 70, 106, and 203 clonal lineages, respectively (Figure 2A). We
178 analyzed the sequences of the HCDR3s and selected HC and LC pairs using IGHD3-15 and having
179 HCDR3 loops longer than 20 amino acids (aa). The core of the macaque IGHD3-15 gene contains a
180 negatively charged motif (see (Figure 2B) that has the capacity to interact with the semi-conserved C-
181 strand of Env V2 (residues 164-172), a region which is often basic in overall charge. [22] These HCDR3
182 features found in RHA1 are characteristic of apex-targeting bNAbs isolated from SHIV-infected NHPs.
183 [24,25] The sequence analysis yielded 16, 30, and 58 HC and LC pairs from the three animals, respectively,
184 that met these antibody signature criteria (Figure 2A).
185
186 Forty-five HC and LC pairs were identified to clone and express as mAbs from NHPs Q9, Q10 and
187 Q12, and their neutralizing activity was assessed on an intial set of tier 2 HIV-1 isolates. This initial
188 panel incorporated viruses from multiple clades that have been termed "apex-sensitive" strains due to
189 their sensitivity of neutralization by the human infection-elicited, apex-directed bNAbs such as PG9/16,
190 PGT145, PGDM1400, VRC26 and others[13,14,35,36]. In a few cases, these isolates are also neutralized by
191 the germline-reverted or UCA variants of the mature apex-directed bNAbs and hence termed apex-
192 sensitive[22,37]. Another characteristic of these isolates is the absence of the N130 glycan, which occupies
193 space adjacent to the N160 glycan on the trimer cap, increasing antibody accessibility to the apex
194 epitopes. In the Seaman 109-virus panel used in a previous report,[22,37,38] 50 isolates lacked this N130
195 glycan. Several of the signature-defined mAbs isolated from NHPs Q9, Q10, and Q12 displayed potent
196 autologous neutralization of the pseudoviruses Q23.17 and ZM233.6. In addition, we detected cross-
197 neutralization of an initial panel of cross-clade HIV-1 clinical isolates (Figure S2A).
198
199 We then selected the broadest mAbs (Figure 2B) from these NHPs and tested them against a larger
200 panel of 64 apex-sensitive viruses, including the infection-elicited apex bNAbs, CH01 and PG9, as
201 comparative controls. The mAbs from NHP Q12 were the most broad and potent, particularly
202 Q12BBM-069, Q12QBM-007, and Q12BBM-023, which neutralized 27, 21, and 22 isolates with
203 median IC_{50} values of 0.5 µg/ml, 1.51 µg/ml, and 0.16 µg/ml, respectively (Figure 2C). The viruses that
204 were not neutralized by these mAbs were further subdivided based on the presence or absence of the
205 N130 glycan (Figure S2B). To note, some Q12 mAbs weakly neutralized the N130 glycan-containing
206 CH505 T/F clinical isolate, but not any other isolates tested that naturally contain this apex N-glycan.
207
208 **Cryo-EM structures reveal that the vaccine-elicited mAbs target the trimer apex like the**
209 **human infection-elicited bNAbs PG9 and CH03**

210

211 We determined high-resolution crystal structures of four Fabs from this set, Q9M-023, Q10M-055,
212 Q12BBM-069 and Q12QBM-007 and observed well-ordered, protruding HCDR3 β-hairpin
213 conformation in three of the four mAbs (Figure S3A, Table S1). To define their epitope specificity at
214 atomic detail, we analyzed these cross-mAbs in complex with NFL trimers by high-resolution cryoEM
215 (Figure S3B, Table S2). CryoEM maps and models of the two most broadly neutralizing mAbs,
216 Q12BBM-069 and Q12QBM-007, in complex with the BG505 NFL trimer, revealed that the vaccine-
217 elicited mAbs bound a quaternary epitope at the trimer apex that greatly overlapped with that of the
218 infection-induced human bNAb PG9 as shown in the BG505 SOSIP:PG9 complex structure (PDB:
219 7T77) (Figure 3A). The epitopes of the NHP mAbs on the trimer surface revealed a similar overall Env
220 contact footprint, especially for the heavy chains, relative to PG9, but with a larger buried surface area
221 (BSA) (Figure 3A). The interactions are dominated by β-hairpin HCDR3 loops that contact the glycans
222 at position N160 in all three protomers, which also occurs with PG9 (Figure 3A). To determine the
223 significance of these antibody-N160 glycan interactions, we generated viruses lacking the N160 glycan
224 by genetically modifying the corresponding potential N-linked glycosylation site (PNGS). We
225 performed a neutralization assay comparing these N160-glycan eliminated viruses to their wild type,
226 N160 glycan-bearing counterparts, observing neutralization dependence on the presence of this glycan,
227 consistent with the apex-directed bNAbs (Figure 3B).[13,14,35] A similar binding pattern and N160 glycan
228 interactions were observed in complexes of Q9M-023 and Q10M-055 with BG505 and Q23 NFL
229 trimers, respectively (Figure S4A). The HCDR3s of all four mAbs adopted a β-hairpin motif that
230 engaged the basic C-strand of Env V2, using both side-chain and backbone interactions, as described
231 for the bNAbs PG9 and CH03 (Figure 4A, S4B). The acidic residues of the HCDR3 make extensive
232 interactions with basic residues in the trimer apex (Figures 4A and S4A). In Q10M-055, a sulfated
233 tyrosine, Y100b, at the tip of the HCDR3 interacts with the Arg169 side-chain and the Asn of N160
234 glycan, stabilizing its HCDR3 loop that is partially disordered in the unliganded crystal structure. This
235 sulfated tyrosine-Env interaction occurs with the most distal Env protomeric unit increasing the
236 antibody's reach despite possessing a shorter HCDR3 (Figure S4A, right panel). A comparison of the
237 cryo-EM structures of the mAbs Q12BBM-069 and Q12QBM-007 trimer complexes and the
238 corresponding unliganded antibody crystal structures suggest that the HCDR3 β-hairpins undergo
239 lateral shifts to avoid steric clashes to facilitate interactions with the N160 glycan and surrounding Env
240 residues (Figure 4B, S4C). This shift varies by antibody, as measured by Cα distance between
241 equivalent residues at the tip of the loop: 7.3 Å (Q12BBM-069), 2.8 Å (Q12QBM-007), and 2.3 Å
242 (Q9M-023), suggesting that the elicited antibodies may have been selected in part for this flexibility,
243 especially Q12BBM-069.
244

245 **HIV Env V2 C-strand mapping analysis provides insights into Ab cross-neutralizing**
246 **specificity**
247 To better understand the neutralization specificities of the cross-reactive mAbs isolated here, we
248 analyzed the sequences of the HIV Env C-strand (residues 164-172) of the N130 glycan-lacking viruses
249 tested in this study. The C-strand amino acid signature of viruses neutralized by Q12BBM-069, the
250 most broadly neutralizing of the antibodies isolated in this study, included the following residues 164E,
251 165L/I, 166R, 167D, 168K/R, 169K/R, 170 Q/R/K, 171K and 172 V/A/E or "$_{164}$ELRDKKQKV$_{172}$"as
252 defined by the most frequent aa at each position. This V2 sequence was highly represented in our series
253 of NFL immunogens. The isolated mAbs make electrostatic interactions with basic amino acids (K/R)
254 often present at four of these aa positions (166, 168, 169 and 171) (Figure 4A). Divergence from this
255 sequence provides natural resistance to neutralization (Figure 4C). This analysis reveals that there is
256 natural resistance in multiple isolates reminiscent of that observed by the apex bNAb VRC26, which
257 does not neutralize clade B viruses. [10] Envs with C strands that differed by two or more positions as
258 defined by the C-strand signature, like that of WITO.33, are neutralization resistant to the NHP
259 antibodies. WITO.33 C-strand aa sequence "$_{164}$VIRDKIQKE$_{172}$" diverges substantially to that of the
260 viruses neutralized by the antibodies isolated here (divergent residues in red).
261
262 While the mAbs characterized here do not neutralize WITO.33, serum IgG from NHPs Q7 and Q8 do
263 neutralize WITO.33, a clade B virus with a divergent V2 C-strand (Figure4D). Mapping the serum IgG
264 from Q7 and Q8 demonstrated that the observed WITO cross-neutralizing activity was directed to the
265 V2 C-strand. Importantly, we precisely mapped this WITO.33 neutralization activities of the Q7 and
266 Q8 serum IgG to the apex by generating WITO.33 C-strand 'knockout' (KO) viral variants that
267 eliminate neutralization activity of apex bNAbs (a double mutant I169E K171E and a single mutant
268 K168E) (Figure 4D). No neutralization activity was observed with either of these KO viruses. In
269 contrast, a single I169R mutation in the divergent WITO.33 V2 sequence increased the neutralization
270 sensitivity to Q7 and Q8 polyclonal IgG, highlighting the importance of the residue 169 in the apex-
271 targeted antibody response elicited in this study. Taken together, these results indicate that
272 neutralization of the divergent clade B WITO.33 virus is directed primarily to the C-strand and that
273 natural resistance afforded by sequence variability in this region can be overcome. This information
274 will guide design of improved immunization regimens based on Env trimer-liposomes. Notably, the
275 serum IgG from NHPs Q9, Q10, and Q12 neutralized viruses 1086c and RW020.2 containing divergent
276 C-strand sequences, indicating the presence of alternate antibody lineages in these NHPs, either directed
277 to the apex or, potentially, targeting other epitopes.
278
279 **Discussion**
280

281 In this study, we describe a vaccine strategy using near-native NFL-stabilized Env trimers covalently
282 arrayed on liposomes that elicited apex-directed cross-neutralizing antibody responses against HIV. Our
283 priming immunogen, Q23 NFL, was identified based on its natural and rare capacity to engage the
284 germline-reverted apex-targeting bNAb RHA1. Sequential heterologous boosting of liposome-arrayed
285 trimers generated cross-neutralizing antibody responses in all NHPs. Following memory B cell sorting
286 with native-like trimers, we isolated mAbs with long, negatively charged HCDR3s (20 residues or
287 longer), typical of apex-targeting NHP bNAbs. We demonstrate that a subset of these mAbs cross-
288 neutralized a large panel of clinical isolates representing different HIV clades. High resolution cryo-
289 EM structures of these antibodies in complex with selected NFL trimers confirms that they target the
290 apex of the HIV-1 Env trimer and display structural features with remarkable similarity to the human
291 infection-elicited bNAbs, PG9 and CH03.
292
293 These results substantially advance efforts in the HIV vaccine field to elicit broadly neutralizing
294 responses directed to the glycan-shielded HIV-1 Env trimer apex beyond the priming of bNAb
295 precursors alone. Typically, the so-called bNAb apex precursors bind to the original engineered
296 germline-targeted trimers but not to more native, wild-type trimers and fail to neutralize wild-type virus.
297 [39] Using germline-guided, natural apex sequence trimers, the results presented here demonstrate that we
298 are able to not just prime apex-directed precursors, but we also educate B cells to take the next several
299 steps by heterologous trimer boosting to drive affinity maturation of apex-directed antibodies that cross-
300 neutralize a wide array of tier 2 cross-clade clinical isolates. The antibodies elicited here recognize wild-
301 type Env, bind and neutralize the autologous viruses already at the post-2 time point, and then mature
302 to develop cross-neutralizing activity following heterologous trimer boosting. We would assert this
303 approach is an alternative to and, in this setting, may be preferable to remodeling the immunogen to
304 become high affinity by altering the Env binding site to increase priming efficiency. Under such
305 circumstances, achieving antibody wild-type Env recognition requires 'boosting energy' to evolve and
306 in the best case, recognize the native Env trimer to achieve neutralization. In contrast, our vaccine
307 strategy efficiently generates antibody responses capable of neutralizing autologous virus immediately
308 following the two 'tandem priming immunogens'.
309
310 The molecular mimicry observed between the vaccine-elicited apex cross-neutralizing mAbs presented
311 here and the infection-driven bNAbs validates our approach. The vaccine-elicited mAbs described in
312 this study successfully engage the N-linked glycan at position 160, an important determinant in
313 neutralization by bNAbs PG9, PGT145, CH01, and CAP256.[22] Extensive engagement of glycans in the
314 HIV Env trimer by cross-neutralizing antibodies is rarely achieved by vaccination.[40] Neutralization
315 primarily of N130 glycan-lacking viruses may be a result of the use of trimer immunogens that also
316 lack this N-glycan, suggesting alternative strategies moving forward. We speculate that by structure-
317 guided immunogen modification it is possible to expand neutralization breadth by using a wider array

318 of C-strand sequences to better evolve this process. In this regard, we detected neutralization of the
319 clade B WITO.33 HIV strain by polyclonal serum IgG from two NHPs, suggesting that this type of
320 antibody evolution by vaccination is possible. The capacity to elicit slightly different specificities in
321 outbred animals shows the potential of the repertoire to elicit many such antibodies from the structural
322 basics of the V2 apex signature with slightly different solutions and the potential to become bNAbs.
323
324 This proof-of-principle study establishes a template for further improvements with this new vaccine-
325 focused positive control system that can be optimized for improvement by head-to-head single variable
326 experiments in NHPs. Transitioning to humans can be accomplished similarly by using UCAs or gL-
327 reverted bNAbs to select natural Env sequences that activate precursor B cells in the human antibody
328 repertoire.
329

330 Resource availability

331

332 Lead contact

333 Information and requests for resources should be directed to and will be fulfilled by the lead contact,
334 Richard T. Wyatt, email – wyatt@scripps.edu
335

336 Materials availability

337 All constructs and antibodies generated in this study are available from the lead contact without
338 restriction.
339

340 **Data and code availability**.
341 The HC VDJ and LC VJ sequences of the Env-specific mAbs have been deposited in GenBank under
342 the codes: For the Heavy Chains: PX281429-PX281473; for the Kappa Chains: PX281474-PX281512;
343 and For the Lambda Chains: PX281513-PX281518. IgM, IgK and IgL repertoire data are available from
344 ENA under the codes: Q9 IGM ERR15498913, Q9 IGK ERR15498914, Q9 IGL ERR15498915, Q10
345 IGM ERR15498916, Q10 IGK ERR15498917, Q10 IGL ERR15498918, Q12 IGM ERR15498919,
346 Q12 IGK ERR15498920, Q12 IGL ERR15498921. The IgDiscover software can be found at
347 https://gkhlab.gitlab.io/igdiscover22/. Cryo-EM maps have been deposited in the Electron Microscopy
348 Data Bank (EMDB) under accession codes EMD-72009, EMD-72031, EMD-72033 and EMD-72035,
349 and cryo-EM models have been deposited in the Protein Data Bank (PDB) under accession codes 9PY5,
350 9PYD, 9PYK and 9PYH. X-ray crystal structures of the Fabs have been deposited in the PDB under
351 the codes 9PYN, 9PYY, 9PZ2 and 9PZ3. Representative negative stain EMPEM maps have been
352 deposited into the Electron Microscopy Data Bank under accession codes EMD-72735, EMD-72736,
353 EMD-72737, EMD-72738 and EMD-72739. All deposited data are publicly available. This paper does

354 not report original code. Any additional information required to reanalyze the data reported in this paper
355 is available from the lead contact upon request.

356 Acknowledgements

357 The work was supported by HIVRAD grants P01 AI104722, P01 AI157299, P01 AI124337, Scripps
358 CHAVD UM1 AI144462 and the James B. Pendleton Trust. This research was funded in part by a
359 Distinguished Professor grant from the Swedish Research Council (agreement number 2017-00968)
360 and the Emory National Primate Research Center Grant Nos. ORIP/ODP51OD011132 and
361 U42PDP11023. The Emory National Primate Center is supported by the National Institutes of Health,
362 Office of Research Infrastructure Programs/OD (P51OD011132 and U42PDP11023). We thank
363 Theresa Fassel from Scripps Research Microscopy Core for assistance in imaging the covalent NFL
364 trimer-liposomes and Raiees Andrabi for confirmatory gl-reverted RHA1.

365

366 Author contributions

367 J.G., S.B., G.B.K.H. and R.T.W. conceived and designed the study. J.G. designed all the immunogens
368 for this study. S.B., J.G., R.T.W. oversaw the immunization studies. S.B. designed the trimer-liposomes
369 and purified the immunogens and trimer-liposomes. R.W. performed serum and IgG neutralization
370 analysis. M.A., F-A.S., I.Z., X.C.D., and M.M. performed IG genotyping, B cell sorting, monoclonal
371 antibody isolation, characterization and engineering. S.P., S.A., G.O., W-H.L., I.A.W. and A.B.W.
372 performed or oversaw the structural analysis. D.C., B.S.H., D.L., V.R.L., D.C. and G.S. oversaw the
373 NHP handling, immunizations, serum and PBMC sample preparation. D.J.I. provided the adjuvant.,
374 S.B., J.G., M.A., G.O., G.B.K.H. and R.T.W. interpreted the results and wrote the manuscript. All
375 authors reviewed, edited and approved the manuscript.

376

377 Declarations of interest

378 D.J.I is an inventor on a patent related to SMNP adjuvant.

379

380 Main figure legends

381

382 **Figure 1. Immunization with NFL trimer-liposomes elicits tier 2 cross-neutralizing antibodies in**
383 **all 6 NHPs.** (A) Surface representation of HIV-1 Env trimer on the membrane (left) and trimer apex
384 (EMD-5273) (right). (B) BLI binding analysis of Q23 and ZM233 NFL trimers to mature RHA1 and
385 inferred germ-line reverted mAbs (igL RHA1). (C) Pictorial representation of liposomes conjugation
386 to trimers (left). Negative stain EM image of trimer-liposome (right). (D) Immunization regimen and
387 NFL trimers used as immunogens. (E) Calcium flux binding response of CH01 UCA to Q23 trimer-
388 liposome or soluble trimer. (F) EMPEM analysis of Q7-Q12 NHPs after immunization with Q23 and

389 ZM233 NFL trimers (P2 bleed). (G) Neutralizing titers against a panel of clinical isolates after
390 immunization with six NFL trimers (P6 bleed). Neutralization experiments were done in duplicate. See
391 also Figure S1.
392
393 **Figure 2. Env-specific memory B cell sorting, sequence analysis and neutralization of apex-**
394 **sensitive clinical isolates by selected mAbs.** (A) Schematic overview of IgG genotyping, Env-specific
395 single memory B cell sorting, analysis of paired HC and LC sequences and expression of mAbs. (B)
396 Genetic properties of mAbs that neutralize more than four HIV-1 strains in the initial panel (Clonally
397 related mAbs are identified with asterisks). D3-15*01 gene central acidic residues are highlighted in
398 red. (C) Neutralizing inhibitory concentrations IC_{50} (μg/mL) for selected mAbs against a sub-panel of
399 27 HIV-1 clinical isolates representing apex-sensitive viruses. The bNAbs RHA1 and PG9 are included
400 for comparison. Neutralization experiments were done in duplicate. See also Figure S2.
401
402 **Figure 3. CryoEM structures of mAbs from Q12 reveal binding at the trimer-apex.** (A) CryoEM
403 maps and models of Q12BBM-069 and Q12QBM-007 Fabs in complex with BG505 NFL compared to
404 a cryoEM model of the bNAb PG9 bound to ApexGT3.N130 BG505 SOSIP trimer (PDB 7T77) (top
405 row). Epitope footprint of mAbs on the surface of Env trimer with buried surface area (BSA)
406 measurements (middle row). Interaction of the HCDR3 loop of the mAbs with glycans at the N160
407 position (blue spheres, bottom row). (B) Neutralizing titers against Q23.17 and BG505.W6M with and
408 without the N160 glycan. Neutralization experiments were done in duplicate. See also Figure S2.
409
410 **Figure 4. Interactions of the HCDR3 loops of NHP mAbs with the V2 C-strand at the trimer apex.**
411 (A) The β-hairpin loops of the HCDR3 of Q12BBM-069 and Q12QBM-007 interact with the C-strand
412 of Env via hydrogen-bonding. Similar interactions are observed for the bNAb PG9 (PDB 7T77) (top
413 row). Key interactions of the HCDR3 tip with the Env trimer-apex (bottom row). (B) Superimposition
414 of the unbound Q12BBM-069 Fab (X-ray) with the bound form (cryoEM). (C) C-strand sequences of
415 viruses neutralized by (left) and not neutralized (right) by Q12BBM-069 (D) Ilustration of PG9 HCDR3
416 interacting with the V2 C-strand of WITO Env (PDB 7T77 and PDB 9BF6) (top). Neutralizing IC_{50}
417 titers against WITO.33 viral variants including C-strand knockout mutant viruses (bottom).
418 Neutralization experiments were done in duplicate. See also Figure S2.

419 # Methods

420

421 ## Ethics statement

422 The animal work was approved by the Emory University Institutional Animal Care and Use Committee
423 (IACUC) under protocol 202100136.

424

425 ## Animals

426 Twelve adult Indian-origin rhesus macaques (*Macaca mulatta*) (RM) were housed at the Emory
427 National Primate Research Center (ENPRC) and maintained in accordance with NIH guidelines.
428 Animal care facilities are accredited by the U.S. Department of Agriculture (USDA) and the Association
429 for Assessment and Accreditation of Laboratory Animal Care (AAALAC) International. Animals were
430 treated with anesthesia (ketamine 5-10 mg/kg or telazol 3-6 mg/kg) and analgesics for procedures
431 including intramuscular (IM) and subcutaneous (SC) immunization, and blood draws as per veterinarian
432 recommendations and IACUC approved protocols. Rhesus macaques were male and female, an age
433 range of 3-4 years old at the start of the study with an average weight of 4.8 kgs. Animals were grouped
434 to divide age and weight as evenly as possible between the groups receiving either soluble or liposome-
435 conjugated trimers. Animals were housed in pairs for the duration of the study.

436

437 ## Cell lines

438 HEK293F cells were cultured in FreeStyle 293 Expression Medium (Thermo Fisher) supplemented
439 with 1x Antibiotic Antimycotic Solution (Sigma-Aldrich) in a humidified incubator (125 rpm, 8% CO_2,
440 37°C). TZM-bl, HEK293T cells were cultured in Dulbecco's modified Eagle Medium (cDMEM)
441 supplemented with 10% fetal Bovine Serum Albumin (BSA) and 1x penicillin-streptomycin-glutamine
442 (Gibco) at 5% CO_2 and 37°C. Expi293F cells were cultured in medium from 293F Expression System
443 Kit in a humidified incubator (125 rpm, 8% CO_2, 37°C).

444

445 ## Design of NFL trimer immunogens and probes

446 The Env sequences used for the generation of the NFL trimeric proteins were derived from the following
447 HIV-1 viral sequences obtained from the Los Alamos National Laboratory HIV sequence database:
448 Q23.17 (AF0048885), ZM233.6 (DQ388517), WITO4160.33 (AY835451), 001428_2 (EF117266),
449 92RW020 (AY669706), BG505.W6M (DQ208456), 16055_2 (EF117268). These DNA sequences
450 were codon optimized to enhance protein expression and modified as follows to make stabilized NFL
451 trimeric Env proteins: the natural HIV-1 leader sequence was replaced by a CD5 leader sequence. The
452 four-residue furin cleavage site $_{508}$REKR$_{511}$ was substituted with a ten-amino acid flexible linker
453 comprising the sequence G_4SG_4S.[26] The C-terminus of the Env sequence was truncated at residue 664
454 resulting in the elimination of the membrane proximal external proximal region (MPER),

455 transmembrane domain (TM), and cytoplasmic tail (CT).[41] An additional linker comprising of residues
456 GGGGSHHHHHHHHGSGC was added to the C-terminus to facilitate coupling to liposomes via the
457 terminal cysteine residue. Finally, a series of stabilizing mutations were introduced to create highly
458 stable and homogeneous trimeric proteins. These stabilizing mutations consist of the TD (BG505
459 Trimer Derived residues), helix-breaking glycine and proline substitutions, unnatural disulfides and V3-
460 loop and Fusion Peptide stabilizing mutations.[27,28,30]
461

462 **Trimer expression, purification, characterization and trimer-liposome preparation**

463 The expression, purification protocols for HIV-1 Env NFL trimers were described in detail
464 previously.[26,28,42,43] NFL trimers used as immunogens were expressed transiently in 293F cells and
465 purified over lectin column followed by negative selection using the non-neutralizing mAb F105
466 followed by size exclusion chromatography (SEC). The trimers were characterized for their structural
467 conformation and antigenicity by SEC, Biolayer interferometry (BLI) and Differential Scanning
468 Calorimetry (DSC). Briefly, the BLI analysis was carried out on an Octet Red instrument (Sartorius)
469 with IgGs immobilized on anti-human IgG Fc capture sensors (Sartorius). The Env trimers were
470 assessed as free analytes in solution (PBS pH 7.4) at a final concentration of 250 nM. Association and
471 dissociation were measured for 60 s respectively. The data were analyzed using ForteBio software
472 version 11.1 and kinetic parameters were obtained using a global 1:1 fit model. The thermal transition
473 temperature (T_m) of the NFL trimers was determined by DSC using a MicroCal VP-Capillary DSC
474 instrument (Malvern Panalytics). The trimer samples were dialyzed in PBS, pH 7.4, and the 400 µl of
475 the trimer sample at concentration of 0.25 mg/mL was loaded into the instrument. The dialysis buffer
476 was used as the reference solution. The DSC experiments were performed at a scanning rate of 1 K/min
477 under 3.0 atmospheres of pressure. The data were analyzed after buffer correction, normalization, and
478 baseline subtraction using MicroCal VP-Capillary DSC analysis software provided by the manufacturer
479 (Origin 7 SR4 v 7.0522). Liposome-conjugated trimers were used as immunogens in NHPs Q7-Q12.
480 The conjugation protocol for generating trimer-liposomes was described in detail previously.[29]
481 Liposomes were comprised of DSPC (1,2-distearoyl-sn-glycero-3-phosphocholine), cholesterol and
482 1,2-dipalmitoyl-*sn*-glycero-3-phosphoethanolamine-N-[4-(p-maleimidomethyl) cyclohexane-
483 carboxamide].[29] Folllowing chemical conjugation with the NFL trimers, the trimer-liposomes were
484 further purified over a Superdex 200 Increase 10/300 GL column in PBS pH 7.4 buffer to remove
485 unconjugated trimers from the trimer-liposomes. The conjugation of trimer to liposomes was confirmed
486 by imaging the trimer-liposomes by a negative stain electron microscope (Scripps Research, EM core).

487 **Calcium Flux**

488 Spleen cells from the CH01ucaDKI mice[44] and the K46 B cell line expressing PG16 [45] were
489 used for the calcium assay. CH01uca cells were suspended at 4 million cells/ml in Advanced
490 DMEM, labeled with 1.5 uM Calbryte™ 520 AM (ATT Bioquest, #20651) with Pluronic™ F-

491 127 (Invitrogen, #P3000MP) for 30 min at 37°C. CH01uca cells were washed with Advanced
492 DMEM and stained with TruStain FcX PLUS (BioLegend, #156604) and Alexa Fluor 647 anti-
493 mouse B220 (BioLegend, #103226) for 10 min at room temperature. Following staining the
494 cells were washed with 2 mM $CaCl_2$ HBSS. After washing, cells were incubated at room
495 temperature for 30 minutes. Two million cells were aliquoted for flow cytometric analysis.
496 Cells were stimulated with NFL trimers or trimer-liposomes, and calcium signals were detected
497 for 240 seconds measuring fluorescence at Ex/Em = 516/533 (B2 peak channel) on a Cytek
498 Aurora spectral flow cytometer (Cytek Biosciences). Analysis was performed using FlowJo
499 (Becton Dickinson). For the PG16 B cell line assay, surface expression of the BCR was induced
500 by adding 1 μg/ml of doxycycline (Thermo Scientific, # J6380506) one day prior. The surface
501 PG16 expression was confirmed by binding of FITC anti-human light chain lambda antibody
502 (BioLegend, #316606) with a Cytek Aurora spectral flow cytometer (Cytek Biosciences).
503 Further confirmation of PG16 surface expression was done by using biotinylated Q23 NFL
504 trimer conjugated to streptavidin-Alexa Fluor 647 (Molecular probes, #S32357). Trimer or
505 trimer-liposome induced calcium flux was measured in a similar way as done for the CH01uca
506 spleen cells.
507
508 **Immunization of NHPs**
509 Twelve NHPs split equally into two groups were inoculated at eight sites (four intramuscular and
510 subcutaneous bi-lateral immunizations on deltoids and inner thighs) with 80 μg of Q23 NFL soluble
511 trimer (NHPs Q1-Q6) or 80 μg of Q23 NFL trimer conjugated to trimer-liposomes (NHPs Q7-Q12) in
512 150 μg SMNP adjuvant. SMNP adjuvant was prepared as previously described[31]. NHPs were
513 immunized with the same formulation (Q23 NFL) at weeks 2, 4, 6 and 8 as a part of the divided-dose
514 regimen. The NHPs were boosted with 150 μg of ZM233 NFL trimer in 375 μg SMNP adjuvant at
515 week 20. Subsequent immunizations with heterologous trimers were performed at 31, 42, and 64 weeks
516 with 100 μg of trimer in 375 μg SMNP adjuvant. Pre-bleeds were collected prior to immunizations and
517 test bleeds were collected on the day of immunizations and 14 days after each immunization. Blood
518 was collected in Na Citrate CPT tubes (BD Biosciences) for peripheral blood mononuclear cells
519 (PBMCs) and plasma isolation. Cells were cryopreserved in FBS with 10% DMSO (Gemini Bio, Fisher
520 Bioreagents). Serum was collected via serum clot tubes (BD Biosciences).
521
522 **Neutralization**
523 Serum IgG was affinity purified with protein A to approximately physiological levels (10mg/mL) as
524 described previously.[30] Replication-incompetent HIV-1 Env pseudoviruses were produced by co-

525 transfecting HEK293T cells with 15 µg of Env-deficient backbone plasmid (pSG3Δ*env*) and 5 µg HIV-
526 1 Env plasmid in a ratio of 1:3 (total DNA: Fugene6 transfection reagent). Pseudoviruses were harvested
527 72 hours after transfection and incubation at 37°C via centrifugation of cell culture supernatants at
528 3000g for 10 minutes and stored at -80°C. Inhibition of entry of HIV-1 Env pseudo-typed viruses into
529 standard TZM-bl cells was used to determine the neutralization capacity of sera, purified total serum
530 IgG or monoclonal antibodies (mAbs) as previously described in a half-well plate format.[46] 50 µL TZM-
531 bl cell suspension (110,000 cells/mL) in cDMEM was added to each well of white, flat-bottomed tissue
532 culture treated plates 24 hrs before setting up the sample dilutions and incubated in a 37°C CO_2
533 incubator. In a 96-well U-bottomed plate, sera, total serum IgG or antibodies were serially diluted in
534 cDMEM five or six times (with 1:3 or 1:5 dilution factors) resulting in a total of six to seven dilution
535 points. In a separate 96-well U-bottomed plate the sample dilutions were mixed with pre-warmed
536 pseudovirus at a ratio of 1 to 5 (6 µL of sample dilution and 24 µL of pseudovirus), resulting in a
537 maximal final serum dilution of 1:10, total serum IgG concentration of 2 mg/mL or antibody
538 concentration of 50 µg/mL. The mixtures were then incubated at 37°C for one hour. cDMEM was then
539 aspirated from the tissue culture plates containing TZM-bl cells, and 25 µL of the sample-pseudovirus
540 mixture was pipetted directly onto the TZM-bl cells and placed in the 37°C incubator for 24 hrs. After
541 24 hrs 75 µL cDMEM was added to all wells of the plates and left at 37°C for another 24 hrs. Finally,
542 the cDMEM/sample mixes were aspirated from the plates, and the TZM-bl cells were lysed for 20
543 minutes on an orbital shaker at 400-500 rpm. Inhibition of entry was determined using the Promega
544 Luciferase system, with luminescence detected by a Biotek NEO2M plate reader. The resulting
545 Luciferase signals were measured in relative light units (RLUs). Sera or antibody dilution that resulted
546 in 50% reduction (ID_{50} values for serum and IC_{50} values for purified IgG or mAbs) in RLUs was
547 determined by fitting the neutralization dose-response curves by non-linear regression using a 5-
548 parameter hill slope equation. Data were analyzed using GraphPad Prism software (version 10.2.1).
549

550 **Individualized immunoglobulin genotyping**

551 To determine the germline V, D and J allele content of the studied rhesus macaque, full-length HC VDJ
552 and LC VJ amplicons were generated as described[33] and analyzed by IgDiscover
553 (https://gkhlab.gitlab.io/igdiscover22/). In brief, total RNA was extracted from approximately 5-10
554 million PBMCs using the Qiagen RNeasy mini kit. 300ng RNA was subjected to reverse transcription
555 with gene-specific primers for the IgM, IgK and IgL constant regions using Sensiscript RT Kit (Qiagen),
556 the cDNA was purified with the Qiagen MinElute PCR Purification Kit and was eluted in 20 µl of
557 elution buffer. 3 µl cDNA were subjected to the library PCR with 25x cycles using multiplex forward
558 VH, VK and VL primer sets and gene-specific primers for the IgM, IgK and IgL constant regions as
559 previously described.[33] The library was gel-purified with Qiagen MinElute Gel Extraction Kit and
560 indexed with 10x PCR cycles following the Illumina MiSeq 2 x 300 bp kit instructions. Indexed library

561 PCR products were purified with MiniElute PCR Purification Kit, followed by AMPure XP magnetic
562 bead (Beckman Coulter) purification prior to sequencing with the Illumina MiSeq 2 x 300 bp kit. The
563 libraries were analyzed using IgDiscover[34] and Corecount[32] to generate HC V, D and J, and LC V and
564 J genotypes. Input databases for the IgDiscover analysis were KIMBD (http://kimdb.gkhlab.se/) for the
565 HC alleles and IMGT for the LC alleles.
566

567 **Env-specific memory B cells sorting by flow cytometry**

568 To produce Env trimer probes for B cell sorting, 10 µg of biotinylated Q23 and BG505 NFL trimers
569 were conjugated to SA-APC (Invitrogen) or SA-BV421 (BioLegend) in five sequential steps, each
570 incubation proceeded for 20 min at 4°C. Frozen single cell suspension from blood mononuclear cells
571 (PBMCs) from animals Q9, Q10, and Q12 were thawed at 37°C, washed twice in pre-warmed RPMI
572 1640 media (HyClone) supplemented with 10% FBS (HyClone) and Penicillin/Streptomycin (100 IU/
573 100 µg/ml) (Gibco). The cells were washed with PBS (Sigma) and counted using trypan blue exclusion
574 of dead cells by a Countess II cell counter (Thermo Fisher). Cells were suspended in PBS and incubated
575 for 30 minutes at 4°C with Live/Dead Fixable Aqua Dead Cell Stain Kit (Life Technologies) according
576 to the manufacturer's instructions. Cells were washed with FACS buffer (PBS + 1% FBS) and surface
577 stained with the following antibodies: CD3 FITC (clone SP34-2), CD14 FITC (clone M5E2), CD20
578 BV421 or PerCP-Cy5.5 (clone 2H7), CD27 PE-Cy7 (clone M-T271), IgG PE-CF594 (clone G18-145)
579 (all from BD Biosciences). Staining was performed for 30 minutes at 4°C. After washing with FACS
580 buffer, cells were subsequently stained with the fluorescently conjugated NFL trimers. Live CD3-
581 CD14-CD20+CD27+IgG+ENV+ single cells were sorted on a four-laser FACSAria Fusion cell sorter
582 (Becton Dickinson) into 96-well PCR plates (Eppendorf) containing 4 µl/well of ice-cold cell lysis
583 buffer (0.5x PBS, 10 mM DTT and 2 U/µl RNAsin (all from Thermo Fisher)). After sorting the 96-well
584 plates were centrifuged, sealed, and immediately frozen on dry ice and stored at -80°C until use.
585

586 **Single B cell RT-PCR and mAb cloning**

587 For cDNA synthesis the 96-well plates, containing single B cells, were thawed on ice. The reverse
588 transcription was performed by SuperScript IV reverse transcriptase (Thermo Fisher) using random
589 hexamers, oligodT, dNTPs (Invitrogen), Igepal CA-630 (Sigma), and RNAsin (Thermo Fisher). IgG
590 HC and LC V(D)J sequences were amplified separately in 20 µl nested PCR reactions using 4 µl of
591 cDNA for HC and 3 µl for LC in the 1st round PCR and 1 µl PCR product in the 2nd round PCR using
592 KAPA HiFi HotStart ReadyMix 2x (Roche). PCR products from positive wells were purified, Sanger
593 sequenced (Genewiz) and analyzed. HC and LC V(D)J sequences were cloned into expression vectors
594 containing the human IgG1, Igκ1, or Igλ2 constant regions. [47], the sequences, engineered with
595 overhangs complementary to the linearized vector ends, were assembled using the Gibson Assembly
596 Master Mix (New England Biolabs). The reaction mixture, consisting of 50 ng of vector and 30 ng of

597 insert in 20 µl reaction mix, was incubated at 50°C for one hour. After incubation, 1 µl of the diluted
598 (1:3) reaction mix was transformed into XL10-Gold ultracompetent cells (Agilent Technologies) by
599 heat shock at 42°C for 30 seconds. Screening of transformed colonies was assessed by PCR, positive
600 clones were expanded, and plasmids were isolated with Plasmid Plus Midi Kit (Qiagen). The correct
601 sequences were confirmed through Sanger sequencing (Genewiz).
602

603 **Monoclonal antibody expression and purification**

604 Monoclonal antibodies (mAbs) were expressed by co-transfecting equal amounts of each HC and LC
605 plasmids (18 µg each) into 30 ml FreeStyle 293-F cells (Thermo Fisher) (HEK293-F) cultured in
606 FreeStyle 293 Expression Medium (Thermo Fisher) supplemented with 1x Antibiotic/Antimycotic
607 solution (Sigma) at a density of 1.2 million cells/ml at >95% viability. Cultures were maintained in a
608 humidified shaking incubator (125 rpm, 8% CO_2, 37°C). Transfections were carried out with FreeStyle
609 Max reagent (Invitrogen) in Opti-MEM medium (Gibco). Seven days after transfection, the mAbs were
610 purified from the supernatant using Protein G Sepharose columns (Cytiva). 4 µg of each purified
611 antibody was analyzed by SDS-PAGE under reducing conditions using NuPAGE 4-12% Bis-Tris
612 polyacrylamide gels (Invitrogen).
613

614 **mAb binding to Env by ELISA**

615 The mAbs were tested for binding to NFL Env trimers. Pierce™ NeutrAvidin™ bovine serum albumin
616 (BSA)-blocked 96-well plates (Thermo Scientific) were coated with 5 µg/ml of NFL trimer, 50 µl/well
617 in wash buffer (25 mM Tris, 150 mM NaCl, pH 7.2; 0.1% BSA, 0.05% Tween-20) for 2 hours.
618 Antibodies, starting at a concentration of 10 µg/ml, were added in 25-fold serial dilutions and incubated
619 for 1 hour at room temperature. The plates were incubated for 45 minutes at room temperature with an
620 HRP-conjugated goat anti-human IgG (H+L) antibody (Jackson ImmunoResearch) diluted 1:10,000 in
621 wash buffer. Each incubation step was followed by six washes with wash buffer. Binding of the mAbs
622 was detected with TMB substrate (Life Technologies) and the reactions were stopped with 1 M sulfuric
623 acid. Optical density (OD) measurements were performed at 450 nm using the Apollo microplate reader
624 (Berthold).
625

626 **Electron-microscopy polyclonal epitope mapping (EMPEM)**

627 Total Serum IgG was digested to polyclonal Fab using papain as per manufacturer's instructions (Pierce
628 Fab Preparation kit, Thermo Scientific). For each immune complex, 1 mg of polyclonal Fab was
629 incubated with 15 µg of Env NFL trimer overnight and purified the next morning using a Cytiva
630 Superdex 200 Increase size-exclusion column. Fractions corresponding to immune complexes were
631 pooled and adsorbed onto 400-mesh carbon-coated copper grids (Electron Microscopy Sciences) at a
632 concentration of ~0.02 mg/mL for 10 s before blotting off the excess liquid. Grids were stained for 45

633 s using 2% (w/v) uranyl formate (Electron Microscopy Sciences) before blotting. Imaging was
634 performed using an Thermo Fisher Scientific Glacios transmission electron microscope operating at
635 200 kV, equipped with Thermo Fisher Scientific Falcon 4 camera (73,000x magnification, 1.89 Å pixel
636 size). Automated data collection was performed using EPU (Thermo Fisher Scientific) and data
637 processing was performed using Relion 4.0[48], following standard procedures. Representative maps have
638 been deposited to the Electron Microscopy Data Bank.
639

640 **Purification and crystallization of unliganded Fabs**

641 Fabs were expressed in Expi293F cells (Thermo Fisher Scientific, Cat. No.: A14527) transiently
642 transfected with plasmid DNA encoding the Fab heavy and light chains at a 1:1 ratio. Transfections
643 were performed using the ExpiFectamine 293 Transfection Kit in Opti-MEM medium. Six days post-
644 transfection, culture supernatants were harvested and sterile filtered through a 0.22 µm membrane filter.
645 Fabs were purified using the CaptureSelect CH1-XL affinity matrix (Thermo Fisher Scientific, Cat.
646 No.: 1943462050), followed by size-exclusion chromatography (SEC) on a Superdex 200 16/600
647 column equilibrated with 20 mM Tris, 150 mM NaCl, pH 7.5. Fractions corresponding to Fab proteins
648 were pooled and concentrated to 12 mg/mL for crystallization. Crystallization screening was performed
649 using our Rigaku CrystalMation robotic system with JCSG Core Suites 1–4, and Top96 Cryo screens
650 at 20°C. Crystals were cryoprotected, if necessary, by supplementing the reservoir solution with 15%
651 ethylene glycol and then flash-cooled in liquid nitrogen for storage prior to data collection.
652

653 **X-ray data collection and structure determination**

654 X-ray diffraction data were collected at beamline 17-ID-1 (AMX) of the National Synchrotron Light
655 Source II. Crystals of Fabs Q9M-023, Q10M-055, Q12QBM-007, and Q12BBM-069 diffracted to
656 resolutions of 2.34 Å, 1.63 Å, 1.54 Å, and 1.79 Å, respectively. The crystallization conditions were as
657 follows: Q9M-023 Fab crystallized in 40% MPD, 0.1 M cacodylate buffer at pH 6.5, and 5% (w/v)
658 PEG-8000; Q10M-055 Fab in 100 mM HEPES at pH 7.5, 10% (v/v) ethylene glycol, and 20% (w/v)
659 PEG-8000; Q12QBM-007 Fab in 50% PEG-200 and 0.1 M citrate at pH 5.5; and Q12BBM-069 Fab in
660 1.26 M ammonium sulfate and 0.1 M cacodylate at pH 6.5. Data processing, including indexing,
661 integration, and scaling, was performed using autoPROC.[49] Structure determination was carried out by
662 molecular replacement using Phaser within the Phenix software suite,[50] with an initial model generated
663 by AlphaFold 3.[51] Subsequent model building and refinement were performed through iterative cycles
664 using Coot and Phenix.refine, respectively.[52,53] The quality of the final structures was assessed using
665 MolProbity,[54] and additional validation was carried out through the PDB validation server. Data
666 collection and refinement statistics are summarized in Table S1.
667

668 **Cryo-electron microscopy**

669 All Fabs used for structural analysis were prepared by cleaving the IgG using papain (Thermo Scientific
670 Cat. #44985). The following four immune complexes were incubated overnight: a) 0.2 mg of BG505
671 NFL TD CC3+ with 0.25 mg of either Q12BBM-069, Q12QBM-007, or Q9M-023; b) 0.2 mg of Q23
672 NFL TD CC3+ with 0.25 mg Q10M-055. Complexes were purified the following morning using a
673 HiLoad 16/600 Superdex 200 pg (Cytiva) gel filtration column. Fractions corresponding to each
674 immune complex were pooled and concentrated using an Amicon 100 kDa MWCO centrifugal device
675 to between 4-6 mg/mL. Samples were vitrified using a Vitrobot Mark IV (Thermo Fisher Scientific).
676 The temperature was set to 4°C and humidity was maintained at 100% during the freezing process. The
677 blotting force was set to 1 and wait time was set to 10 s. Blotting time was varied from 3 to 6 s. Detergent
678 lauryl maltose neopentyl glycol (LMNG; Anatrace) was added to the sample to a final concentration of
679 0.005 mM shortly before freezing. UltrAuFoil 1.2/1.3 (Au, 300-mesh; Quantifoil Micro Tools GmbH)
680 grids were used and glow discharged (PELCO easiGlow, Ted Pella, Inc.) for 40 s prior to sample
681 application. 0.5 µL of detergent was mixed with 3.5 µL of samples and 3 µL of the mixture was
682 immediately loaded onto the grid. Following blotting, the grids were plunge-frozen into liquid nitrogen-
683 cooled liquid ethane.
684 Samples were loaded into a Thermo Fisher Scientific Glacios 2 TEM operating at 200 kV equipped
685 with a Thermo Fisher Scientific Falcon 4i direct electron detector. Exposure magnification was set to
686 190,000x with a pixel size at the specimen plane of 0.718 Å. EPU software (Thermo Fisher Scientific)
687 was used for automated data collection. Micrograph movie frames were motion corrected, dose
688 weighted, and CTF correction was performed using cryoSPARC Live.[55] cryoSPARC was used for the
689 remainder of data processing**.** Particle picking was performed using blob picker initially followed by
690 template picker. Particles were initially down-sampled by a factor of 4 and multiple rounds of 2D
691 classification were performed followed by 3D ab initio reconstruction. The remaining particles were
692 then re-extracted, with optional Fourier cropping to reduce memory requirements of large box sizes,
693 resulting in image pixel sizes of 1.034 Å (Q12BBM-069 + BG505), 1.005 Å (Q12QBM-007 + BG505),
694 0.718 Å (Q9M-023 + BG505) or 1.034 Å (Q10M-055 + Q23). 3D non-uniform refinement was
695 performed. For all cryo-EM maps, global resolution was estimated using half maps and a Fourier shell
696 correlation cutoff of 0.143, and local resolution estimated using the cryoSPARC Local Resolution tool
697 with 0.143 FSC cutoff.
698 Initial models were generated using AlphaFold3 and docked into the cryo-EM maps using UCSF
699 ChimeraX.[51,56] Manual building was performed in Coot 0.9.8 and real space refinement in Phenix.[57,58]
700 Final models were validated using MolProbity and EMRinger in the Phenix suite. Buried surface area
701 calculations and interface analyses were performed using UCSF ChimeraX. Data collection, processing
702 and model statistics are summarized in Figure S3 and Table S2.
703
704 **Supplementary Information**

705 Document S1. Figures S1-S4

706 Table S1. X-ray data collection and refinement statistics.

707 Table S2. Cryo-EM data collection, refinement and validation statistics, related to Figure 3.

708

709 **References**

710

711 1. Kirchhoff, F. (2010). Immune evasion and counteraction of restriction factors by HIV-
712 1 and other primate lentiviruses. Cell Host Microbe *8*, 55-67.
713 10.1016/j.chom.2010.06.004.
714 2. Masenga, S.K., Mweene, B.C., Luwaya, E., Muchaili, L., Chona, M., and Kirabo, A.
715 (2023). HIV-Host Cell Interactions. Cells *12*. 10.3390/cells12101351.
716 3. Kulpa, D.A., Paiardini, M., and Silvestri, G. (2025). Immune-mediated strategies to
717 solving the HIV reservoir problem. Nat Rev Immunol *25*, 542-553. 10.1038/s41577-
718 025-01136-7.
719 4. Starcich, B.R., Hahn, B.H., Shaw, G.M., McNeely, P.D., Modrow, S., Wolf, H., Parks,
720 E.S., Parks, W.P., Josephs, S.F., Gallo, R.C., and et al. (1986). Identification and
721 characterization of conserved and variable regions in the envelope gene of HTLV-
722 III/LAV, the retrovirus of AIDS. Cell *45*, 637-648. 10.1016/0092-8674(86)90778-6.
723 5. Wei, X., Decker, J.M., Wang, S., Hui, H., Kappes, J.C., Wu, X., Salazar-Gonzalez, J.F.,
724 Salazar, M.G., Kilby, J.M., Saag, M.S., et al. (2003). Antibody neutralization and
725 escape by HIV-1. Nature *422*, 307-312.
726 6. Crispin, M., Ward, A.B., and Wilson, I.A. (2018). Structure and Immune Recognition
727 of the HIV Glycan Shield. Annu Rev Biophys *47*, 499-523. 10.1146/annurev-biophys-
728 060414-034156.
729 7. McCoy, L.E., and Burton, D.R. (2017). Identification and specificity of broadly
730 neutralizing antibodies against HIV. Immunol Rev *275*, 11-20. 10.1111/imr.12484.
731 8. Willis, J.R., Berndsen, Z.T., Ma, K.M., Steichen, J.M., Schiffner, T., Landais, E.,
732 Liguori, A., Kalyuzhniy, O., Allen, J.D., Baboo, S., et al. (2022). Human
733 immunoglobulin repertoire analysis guides design of vaccine priming immunogens
734 targeting HIV V2-apex broadly neutralizing antibody precursors. Immunity *55*, 2149-
735 2167 e2149. 10.1016/j.immuni.2022.09.001.
736 9. Bonsignori, M., Hwang, K.K., Chen, X., Tsao, C.Y., Morris, L., Gray, E., Marshall,
737 D.J., Crump, J.A., Kapiga, S.H., Sam, N.E., et al. (2011). Analysis of a clonal lineage
738 of HIV-1 envelope V2/V3 conformational epitope-specific broadly neutralizing
739 antibodies and their inferred unmutated common ancestors. J Virol *85*, 9998-10009.
740 10.1128/JVI.05045-11.
741 10. Doria-Rose, N.A., Bhiman, J.N., Roark, R.S., Schramm, C.A., Gorman, J., Chuang,
742 G.Y., Pancera, M., Cale, E.M., Ernandes, M.J., Louder, M.K., et al. (2016). New
743 Member of the V1V2-Directed CAP256-VRC26 Lineage That Shows Increased
744 Breadth and Exceptional Potency. J Virol *90*, 76-91. 10.1128/JVI.01791-15.
745 11. Doria-Rose, N.A., Schramm, C.A., Gorman, J., Moore, P.L., Bhiman, J.N., DeKosky,
746 B.J., Ernandes, M.J., Georgiev, I.S., Kim, H.J., Pancera, M., et al. (2014).
747 Developmental pathway for potent V1V2-directed HIV-neutralizing antibodies. Nature
748 *509*, 55-62. 10.1038/nature13036.
749 12. Landais, E., Murrell, B., Briney, B., Murrell, S., Rantalainen, K., Berndsen, Z.T.,
750 Ramos, A., Wickramasinghe, L., Smith, M.L., Eren, K., et al. (2017). HIV Envelope
751 Glycoform Heterogeneity and Localized Diversity Govern the Initiation and

752 Maturation of a V2 Apex Broadly Neutralizing Antibody Lineage. Immunity *47*, 990-
753 1003 e1009. 10.1016/j.immuni.2017.11.002.
754 13. Sok, D., van Gils, M.J., Pauthner, M., Julien, J.P., Saye-Francisco, K.L., Hsueh, J.,
755 Briney, B., Lee, J.H., Le, K.M., Lee, P.S., et al. (2014). Recombinant HIV envelope
756 trimer selects for quaternary-dependent antibodies targeting the trimer apex. Proc Natl
757 Acad Sci U S A *111*, 17624-17629. 10.1073/pnas.1415789111.
758 14. Walker, L.M., Huber, M., Doores, K.J., Falkowska, E., Pejchal, R., Julien, J.P., Wang,
759 S.K., Ramos, A., Chan-Hui, P.Y., Moyle, M., et al. (2011). Broad neutralization
760 coverage of HIV by multiple highly potent antibodies. Nature *477*, 466-470.
761 10.1038/nature10373.
762 15. Walker, L.M., Phogat, S.K., Chan-Hui, P.Y., Wagner, D., Phung, P., Goss, J.L., Wrin,
763 T., Simek, M.D., Fling, S., Mitcham, J.L., et al. (2009). Broad and potent neutralizing
764 antibodies from an African donor reveal a new HIV-1 vaccine target. Science *326*, 285-
765 289. 10.1126/science.1178746.
766 16. Pancera, M., McLellan, J.S., Wu, X., Zhu, J., Changela, A., Schmidt, S.D., Yang, Y.,
767 Zhou, T., Phogat, S., Mascola, J.R., and Kwong, P.D. (2010). Crystal structure of PG16
768 and chimeric dissection with somatically related PG9: structure-function analysis of
769 two quaternary-specific antibodies that effectively neutralize HIV-1. J Virol *84*, 8098-
770 8110. 10.1128/jvi.00966-10.
771 17. McLellan, J.S., Pancera, M., Carrico, C., Gorman, J., Julien, J.P., Khayat, R., Louder,
772 R., Pejchal, R., Sastry, M., Dai, K., et al. (2011). Structure of HIV-1 gp120 V1/V2
773 domain with broadly neutralizing antibody PG9. Nature *480*, 336-343.
774 10.1038/nature10696.
775 18. Lee, J.H., Andrabi, R., Su, C.Y., Yasmeen, A., Julien, J.P., Kong, L., Wu, N.C.,
776 McBride, R., Sok, D., Pauthner, M., et al. (2017). A Broadly Neutralizing Antibody
777 Targets the Dynamic HIV Envelope Trimer Apex via a Long, Rigidified, and Anionic
778 beta-Hairpin Structure. Immunity *46*, 690-702. 10.1016/j.immuni.2017.03.017.
779 19. Gorman, J., Chuang, G.Y., Lai, Y.T., Shen, C.H., Boyington, J.C., Druz, A., Geng, H.,
780 Louder, M.K., McKee, K., Rawi, R., et al. (2020). Structure of Super-Potent Antibody
781 CAP256-VRC26.25 in Complex with HIV-1 Envelope Reveals a Combined Mode of
782 Trimer-Apex Recognition. Cell reports *31*, 107488. 10.1016/j.celrep.2020.03.052.
783 20. Gorman, J., Soto, C., Yang, M.M., Davenport, T.M., Guttman, M., Bailer, R.T.,
784 Chambers, M., Chuang, G.Y., DeKosky, B.J., Doria-Rose, N.A., et al. (2016).
785 Structures of HIV-1 Env V1V2 with broadly neutralizing antibodies reveal
786 commonalities that enable vaccine design. Nat Struct Mol Biol *23*, 81-90.
787 10.1038/nsmb.3144.
788 21. Andrabi, R., Su, C.Y., Liang, C.H., Shivatare, S.S., Briney, B., Voss, J.E., Nawazi,
789 S.K., Wu, C.Y., Wong, C.H., and Burton, D.R. (2017). Glycans Function as Anchors
790 for Antibodies and Help Drive HIV Broadly Neutralizing Antibody Development.
791 Immunity *47*, 1004. 10.1016/j.immuni.2017.10.012.
792 22. Andrabi, R., Voss, J.E., Liang, C.H., Briney, B., McCoy, L.E., Wu, C.Y., Wong, C.H.,
793 Poignard, P., and Burton, D.R. (2015). Identification of Common Features in Prototype
794 Broadly Neutralizing Antibodies to HIV Envelope V2 Apex to Facilitate Vaccine
795 Design. Immunity *43*, 959-973. 10.1016/j.immuni.2015.10.014.
796 23. Rantalainen, K., Berndsen, Z.T., Murrell, S., Cao, L., Omorodion, O., Torres, J.L., Wu,
797 M., Umotoy, J., Copps, J., Poignard, P., et al. (2018). Co-evolution of HIV Envelope
798 and Apex-Targeting Neutralizing Antibody Lineage Provides Benchmarks for Vaccine
799 Design. Cell Rep *23*, 3249-3261. 10.1016/j.celrep.2018.05.046.
800 24. Roark, R.S., Li, H., Williams, W.B., Chug, H., Mason, R.D., Gorman, J., Wang, S.,
801 Lee, F.H., Rando, J., Bonsignori, M., et al. (2021). Recapitulation of HIV-1 Env-

802 antibody coevolution in macaques leading to neutralization breadth. Science *371*.
803 10.1126/science.abd2638.
804 25. Roark, R.S., Habib, R., Gorman, J., Li, H., Connell, A.J., Bonsignori, M., Guo, Y.,
805 Hogarty, M.P., Olia, A.S., Sowers, K.J., et al. (2025). Structural and genetic basis of
806 HIV-1 envelope V2 apex recognition by rhesus broadly neutralizing antibodies. J Exp
807 Med *222*. 10.1084/jem.20250638.
808 26. Sharma, S.K., de Val, N., Bale, S., Guenaga, J., Tran, K., Feng, Y., Dubrovskaya, V.,
809 Ward, A.B., and Wyatt, R.T. (2015). Cleavage-independent HIV-1 Env trimers
810 engineered as soluble native spike mimetics for vaccine design. Cell reports *11*, 539-
811 550. 10.1016/j.celrep.2015.03.047.
812 27. Guenaga, J., Dubrovskaya, V., de Val, N., Sharma, S.K., Carrette, B., Ward, A.B., and
813 Wyatt, R.T. (2015). Structure-Guided Redesign Increases the Propensity of HIV Env
814 To Generate Highly Stable Soluble Trimers. J Virol *90*, 2806-2817.
815 10.1128/JVI.02652-15.
816 28. Guenaga, J., Garces, F., de Val, N., Stanfield, R.L., Dubrovskaya, V., Higgins, B.,
817 Carrette, B., Ward, A.B., Wilson, I.A., and Wyatt, R.T. (2017). Glycine Substitution at
818 Helix-to-Coil Transitions Facilitates the Structural Determination of a Stabilized
819 Subtype C HIV Envelope Glycoprotein. Immunity *46*, 792-803 e793.
820 10.1016/j.immuni.2017.04.014.
821 29. Bale, S., Goebrecht, G., Stano, A., Wilson, R., Ota, T., Tran, K., Ingale, J., Zwick, M.B.,
822 and Wyatt, R.T. (2017). Covalent Linkage of HIV-1 Trimers to Synthetic Liposomes
823 Elicits Improved B Cell and Antibody Responses. J Virol *91*. 10.1128/JVI.00443-17.
824 30. Schleich, F.A., Bale, S., Guenaga, J., Ozorowski, G., Adori, M., Lin, X., Castro Dopico,
825 X., Wilson, R., Chernyshev, M., Cotgreave, A.T., et al. (2025). Vaccination of
826 nonhuman primates elicits a broadly neutralizing antibody lineage targeting a
827 quaternary epitope on the HIV-1 Env trimer. Immunity *58*, 1598-1613 e1598.
828 10.1016/j.immuni.2025.04.010.
829 31. Silva, M., Kato, Y., Melo, M.B., Phung, I., Freeman, B.L., Li, Z., Roh, K., Van
830 Wijnbergen, J.W., Watkins, H., Enemuo, C.A., et al. (2021). A particulate saponin/TLR
831 agonist vaccine adjuvant alters lymph flow and modulates adaptive immunity. Sci
832 Immunol *6*, eabf1152. 10.1126/sciimmunol.abf1152.
833 32. Narang, S., Kaduk, M., Chernyshev, M., Karlsson Hedestam, G.B., and Corcoran,
834 M.M. (2023). Adaptive immune receptor genotyping using the corecount program.
835 Frontiers in immunology *14*, 1125884. 10.3389/fimmu.2023.1125884.
836 33. Mandolesi, M., Das, H., de Vries, L., Yang, Y., Kim, C., Dhinakaran, M., Castro
837 Dopico, X., Fischbach, J., Kim, S., Guryleva, M.V., et al. (2024). Multi-compartmental
838 diversification of neutralizing antibody lineages dissected in SARS-CoV-2 spike-
839 immunized macaques. Nature communications *15*, 6338. 10.1038/s41467-024-50286-
840 0.
841 34. Corcoran, M.M., Phad, G.E., Vazquez Bernat, N., Stahl-Hennig, C., Sumida, N.,
842 Persson, M.A., Martin, M., and Karlsson Hedestam, G.B. (2016). Production of
843 individualized V gene databases reveals high levels of immunoglobulin genetic
844 diversity. Nature communications *7*, 13642. 10.1038/ncomms13642.
845 35. Walker, L.M., Phogat, S.K., Chan-Hui, P.Y., Wagner, D., Phung, P., Goss, J.L., Wrin,
846 T., Simek, M.D., Fling, S., Mitcham, J.L., et al. (2009). Broad and potent neutralizing
847 antibodies from an African donor reveal a new HIV-1 vaccine target. Science *326*, 285-
848 289.
849 36. Doria-Rose, N.A., Schramm, C.A., Gorman, J., Moore, P.L., Bhiman, J.N., Dekosky,
850 B.J., Ernandes, M.J., Georgiev, I.S., Kim, H.J., Pancera, M., et al. (2014).

851 Developmental pathway for potent V1V2-directed HIV-neutralizing antibodies. Nature
852 *509*, 55-62. 10.1038/nature13036.
853 37. Voss, J.E., Andrabi, R., McCoy, L.E., de Val, N., Fuller, R.P., Messmer, T., Su, C.Y.,
854 Sok, D., Khan, S.N., Garces, F., et al. (2017). Elicitation of Neutralizing Antibodies
855 Targeting the V2 Apex of the HIV Envelope Trimer in a Wild-Type Animal Model.
856 Cell reports *21*, 222-235. 10.1016/j.celrep.2017.09.024.
857 38. Seaman, M.S., Janes, H., Hawkins, N., Grandpre, L.E., Devoy, C., Giri, A., Coffey,
858 R.T., Harris, L., Wood, B., Daniels, M.G., et al. (2010). Tiered categorization of a
859 diverse panel of HIV-1 Env pseudoviruses for assessment of neutralizing antibodies. J
860 Virol *84*, 1439-1452. 10.1128/JVI.02108-09.
861 39. Ma, K.M., Sutton, H.J., Pratap, P.P., Steichen, J.M., Carnathan, D., Quinn, J.,
862 Kalyuzhniy, O., Liguori, A., Agrawal, S., Baboo, S., et al. (2025). HIV broadly
863 neutralizing antibody precursors to the Apex epitope induced in nonhuman primates.
864 Sci Immunol *10*, eadt6660. 10.1126/sciimmunol.adt6660.
865 40. Dubrovskaya, V., Tran, K., Ozorowski, G., Guenaga, J., Wilson, R., Bale, S., Cottrell,
866 C.A., Turner, H.L., Seabright, G., O'Dell, S., et al. (2019). Vaccination with Glycan-
867 Modified HIV NFL Envelope Trimer-Liposomes Elicits Broadly Neutralizing
868 Antibodies to Multiple Sites of Vulnerability. Immunity *51*, 915-929 e917.
869 10.1016/j.immuni.2019.10.008.
870 41. Klasse, P.J., Ketas, T.J., Cottrell, C.A., Ozorowski, G., Debnath, G., Camara, D.,
871 Francomano, E., Pugach, P., Ringe, R.P., LaBranche, C.C., et al. (2018). Epitopes for
872 neutralizing antibodies induced by HIV-1 envelope glycoprotein BG505 SOSIP trimers
873 in rabbits and macaques. PLoS Pathog *14*, e1006913. 10.1371/journal.ppat.1006913.
874 42. Dubrovskaya, V., Guenaga, J., de Val, N., Wilson, R., Feng, Y., Movsesyan, A.,
875 Karlsson Hedestam, G.B., Ward, A.B., and Wyatt, R.T. (2017). Targeted N-glycan
876 deletion at the receptor-binding site retains HIV Env NFL trimer integrity and
877 accelerates the elicited antibody response. PLoS Pathog *13*, e1006614.
878 10.1371/journal.ppat.1006614.
879 43. Guenaga, J., de Val, N., Tran, K., Feng, Y., Satchwell, K., Ward, A.B., and Wyatt, R.T.
880 (2015). Well-Ordered Trimeric HIV-1 Subtype B and C Soluble Spike Mimetics
881 Generated by Negative Selection Display Native-like Properties. PLoS Pathog *11*,
882 e1004570. 10.1371/journal.ppat.1004570.
883 44. Williams, W.B., Zhang, J., Jiang, C., Nicely, N.I., Fera, D., Luo, K., Moody, M.A.,
884 Liao, H.X., Alam, S.M., Kepler, T.B., et al. (2017). Initiation of HIV neutralizing B
885 cell lineages with sequential envelope immunizations. Nature communications *8*, 1732.
886 10.1038/s41467-017-01336-3.
887 45. Ota, T., Doyle-Cooper, C., Cooper, A.B., Huber, M., Falkowska, E., Doores, K.J.,
888 Hangartner, L., Le, K., Sok, D., Jardine, J., et al. (2012). Anti-HIV B Cell lines as
889 candidate vaccine biosensors. J Immunol *189*, 4816-4824. 10.4049/jimmunol.1202165.
890 46. Landais, E., Huang, X., Havenar-Daughton, C., Murrell, B., Price, M.A.,
891 Wickramasinghe, L., Ramos, A., Bian, C.B., Simek, M., Allen, S., et al. (2016). Broadly
892 Neutralizing Antibody Responses in a Large Longitudinal Sub-Saharan HIV Primary
893 Infection Cohort. PLoS Pathog *12*, e1005369. 10.1371/journal.ppat.1005369.
894 47. Tiller, T., Meffre, E., Yurasov, S., Tsuiji, M., Nussenzweig, M.C., and Wardemann, H.
895 (2008). Efficient generation of monoclonal antibodies from single human B cells by
896 single cell RT-PCR and expression vector cloning. J Immunol Methods *329*, 112-124.
897 10.1016/j.jim.2007.09.017.
898 48. Zivanov, J., Nakane, T., Forsberg, B.O., Kimanius, D., Hagen, W.J., Lindahl, E., and
899 Scheres, S.H. (2018). New tools for automated high-resolution cryo-EM structure
900 determination in RELION-3. eLife *7*. 10.7554/eLife.42166.

49. Vonrhein, C., Flensburg, C., Keller, P., Sharff, A., Smart, O., Paciorek, W., Womack, T., and Bricogne, G. (2011). Data processing and analysis with the autoPROC toolbox. Acta Crystallogr D Biol Crystallogr *67*, 293-302. 10.1107/S0907444911007773.
50. McCoy, A.J., Grosse-Kunstleve, R.W., Adams, P.D., Winn, M.D., Storoni, L.C., and Read, R.J. (2007). Phaser crystallographic software. J Appl Crystallogr *40*, 658-674. 10.1107/S0021889807021206.
51. Abramson, J., Adler, J., Dunger, J., Evans, R., Green, T., Pritzel, A., Ronneberger, O., Willmore, L., Ballard, A.J., Bambrick, J., et al. (2024). Accurate structure prediction of biomolecular interactions with AlphaFold 3. Nature *630*, 493-500. 10.1038/s41586-024-07487-w.
52. Afonine, P.V., Grosse-Kunstleve, R.W., Echols, N., Headd, J.J., Moriarty, N.W., Mustyakimov, M., Terwilliger, T.C., Urzhumtsev, A., Zwart, P.H., and Adams, P.D. (2012). Towards automated crystallographic structure refinement with phenix.refine. Acta Crystallogr D Biol Crystallogr *68*, 352-367. 10.1107/S0907444912001308.
53. Emsley, P., Lohkamp, B., Scott, W.G., and Cowtan, K. (2010). Features and development of Coot. Acta Crystallogr D Biol Crystallogr *66*, 486-501. 10.1107/S0907444910007493.
54. Chen, V.B., Arendall, W.B., 3rd, Headd, J.J., Keedy, D.A., Immormino, R.M., Kapral, G.J., Murray, L.W., Richardson, J.S., and Richardson, D.C. (2010). MolProbity: all-atom structure validation for macromolecular crystallography. Acta Crystallogr D Biol Crystallogr *66*, 12-21. 10.1107/S0907444909042073.
55. Punjani, A., Rubinstein, J.L., Fleet, D.J., and Brubaker, M.A. (2017). cryoSPARC: algorithms for rapid unsupervised cryo-EM structure determination. Nat Methods *14*, 290-296. 10.1038/nmeth.4169.
56. Meng, E.C., Goddard, T.D., Pettersen, E.F., Couch, G.S., Pearson, Z.J., Morris, J.H., and Ferrin, T.E. (2023). UCSF ChimeraX: Tools for structure building and analysis. Protein Sci *32*, e4792. 10.1002/pro.4792.
57. Casanal, A., Lohkamp, B., and Emsley, P. (2020). Current developments in Coot for macromolecular model building of Electron Cryo-microscopy and Crystallographic Data. Protein Sci *29*, 1069-1078. 10.1002/pro.3791.
58. Liebschner, D., Afonine, P.V., Baker, M.L., Bunkoczi, G., Chen, V.B., Croll, T.I., Hintze, B., Hung, L.W., Jain, S., McCoy, A.J., et al. (2019). Macromolecular structure determination using X-rays, neutrons and electrons: recent developments in Phenix. Acta Crystallogr D Struct Biol *75*, 861-877. 10.1107/S2059798319011471.
59. Vazquez Bernat, N., Corcoran, M., Hardt, U., Kaduk, M., Phad, G.E., Martin, M., and Karlsson Hedestam, G.B. (2019). High-Quality Library Preparation for NGS-Based Immunoglobulin Germline Gene Inference and Repertoire Expression Analysis. Front Immunol *10*, 660. 10.3389/fimmu.2019.00660.
60. Schritt, D., Li, S., Rozewicki, J., Katoh, K., Yamashita, K., Volkmuth, W., Cavet, G., and Standley, D.M. (2019). Repertoire Builder: high-throughput structural modeling of B and T cell receptors. Molecular Systems Design & Engineering *4*, 761-768. 10.1039/C9ME00020H.
61. Pettersen, E.F., Goddard, T.D., Huang, C.C., Couch, G.S., Greenblatt, D.M., Meng, E.C., and Ferrin, T.E. (2004). UCSF Chimera--a visualization system for exploratory research and analysis. Journal of computational chemistry *25*, 1605-1612. 10.1002/jcc.20084.
62. Goddard, T.D., Huang, C.C., Meng, E.C., Pettersen, E.F., Couch, G.S., Morris, J.H., and Ferrin, T.E. (2018). UCSF ChimeraX: Meeting modern challenges in visualization and analysis. Protein Sci *27*, 14-25. 10.1002/pro.3235.

950 63. Suloway, C., Pulokas, J., Fellmann, D., Cheng, A., Guerra, F., Quispe, J., Stagg, S.,
951 Potter, C.S., and Carragher, B. (2005). Automated molecular microscopy: the new
952 Leginon system. Journal of structural biology *151*, 41-60. 10.1016/j.jsb.2005.03.010.
953 64. Zhang, J., Kobert, K., Flouri, T., and Stamatakis, A. (2014). PEAR: a fast and accurate
954 Illumina Paired-End reAd mergeR. Bioinformatics *30*, 614-620.
955 10.1093/bioinformatics/btt593.
956

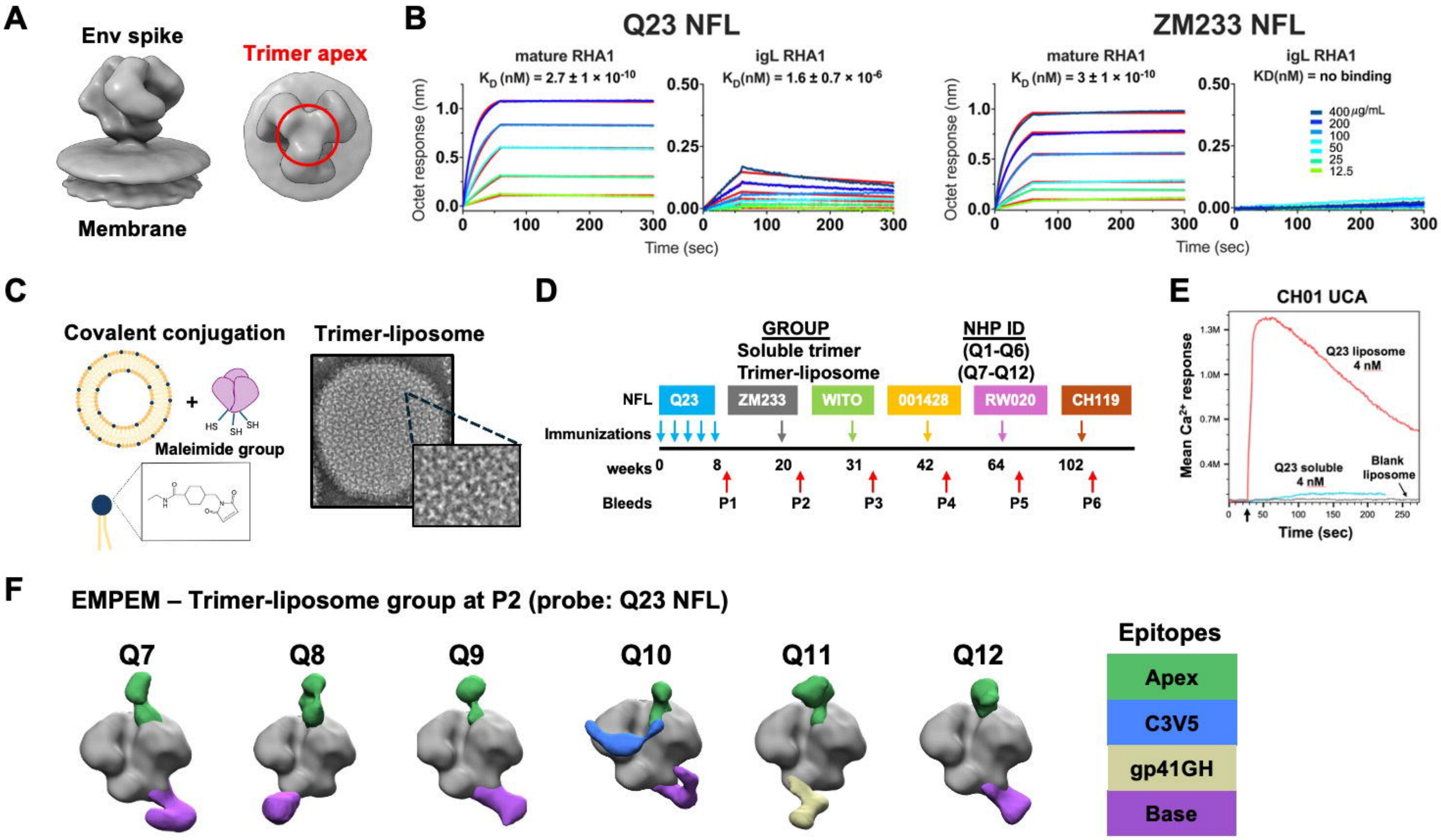

G Serum IgG HIV-1 neutralization at P6

Virus	Soluble trimer Q1	Q2	Q3	Q4	Q5	Q6	Trimer-liposome Q7	Q8	Q9	Q10	Q11	Q12
Q23_17	87	29	23	25	236	881	7	3	<2	14	13	<2
ZM233_6	45	13	4	45	84	98	95	<2	<2	3	3	<2
001428_2_42	126	120	68	58	128	404	351	84	47	363	145	6
C1080.c3	72	147	175	157	847	686	5	14	62	84	94	25
16055_2_3	-	238	-	-	-	-	72	10	10	535	1675	14
1086c	-	-	-	-	-	-	470	308	188	510	480	19
CAP45_G3	-	458	-	-	-	-	60	45	360	67	481	39
BG505.W6M.C2	-	1211	-	-	-	-	380	49	12	-	-	8
BJOX20000	-	-	-	-	-	-	-	111	16	510	-	28
JR-FL.JB	-	746	-	-	-	-	-	-	-	-	774	669
25710_2_43	680	261	325	-	-	560	353	451	146	742	85	57
T250-4	428	110	-	-	-	-	142	49	161	223	647	15
RW020.2	-	621	519	-	-	-	520	861	684	715	424	-
WITO.33	-	-	-	-	-	-	102	184	-	-	-	-
CAP256	-	-	-	-	-	-	-	282	-	-	-	-
CE1176	-	-	-	-	-	-	1486	797	-	-	-	-
X1632	-	-	-	-	-	-	823	-	-	-	534	-
Sc422_8	-	-	-	-	-	-	-	-	-	-	-	-
Pt45.G5	-	-	-	-	-	-	-	-	-	-	-	-
SIV251	-	-	-	-	-	-	-	-	-	-	-	-
VSV	-	-	-	-	-	-	-	-	-	-	-	-

IgG IC_{50} (μg/ml)

>300
30-300
3-30
<3

Figure 1

A

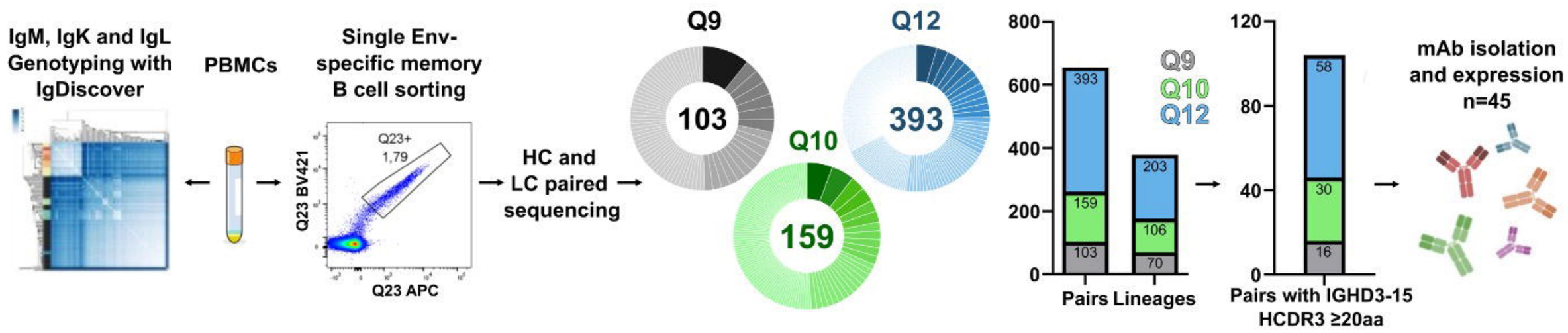

B

NHP ID	mAb ID	IGHV allele	IGHD allele	IGHJ allele	HCDR3	HCDR3 length	% VH SHM nt	% VH SHM aa	IGKV/IGLV allele	IGKJ/IGLJ allele
Q9	Q9M-023	IGHV4-117*01	IGHD3-15*01	IGHJ3-2*01	ARPVRADHEDDDGYYYSYDDAFDL	24	8.8	13.3	IGKV1-21*01_kim	IGKJ2*01
Q10	Q10M-054*	IGHV4-117*01_S8404	IGHD3-15*01	IGHJ3-2*01	ASDLYYEDDDGYSYEGLDVFDF	22	12.8	19.4	IGKV3-42*02_kim	IGKJ1*01
	Q10M-055*	IGHV4-117*01_S8404	IGHD3-15*01	IGHJ3-2*01	ASDLYYEDDYGYSYEGLDVFDF	22	8.8	16.3	IGKV3-42*02_kim	IGKJ1*01
	Q10M-100**	IGHV4-117*01	IGHD3-15*01	IGHJ5-4*02	ARDGTYYDDDDGYYYTDQWFNV	22	8.8	16.3	IGKV3-42*02_kim	IGKJ1*01
	Q10M-123**	IGHV4-117*01	IGHD3-15*01	IGHJ5-4*02	ARDGTYYDDDDGYYYTDNWFNV	22	10.1	15.3	IGKV3-42*02_kim	IGKJ1*01
Q12	Q12M-032***	IGHV4-117*01	IGHD3-15*01	IGHJ2*01	AKEALRGYEDEFDGYYTLNDFYFDV	25	7.8	14.3	IGKV1-25*01_kim	IGKJ4*01
	Q12QBM-007***	IGHV4-117*01	IGHD3-15*01	IGHJ2*01	AKEAIRGYEDEFDGYYTLNDYYYDV	25	7.2	15.5	IGKV1-25*01_kim	IGKJ4*01
	Q12BBM-023***	IGHV4-117*01	IGHD3-15*01	IGHJ2*01	AKEAIRGYEDEFDGYYTLNDWYFDV	25	9.1	17.3	IGKV1-25*01_kim	IGKJ4*01
	Q12BBM-069	IGHV4-174*01	IGHD3-15*01	IGHJ2*01	TKDAIRGYEDEFDGYYTLNDFYFDV	25	10.8	21.4	IGKV1-25*01_kim	IGKJ4*01

C HIV-1 cross-neutralization of mAbs

				Vaccine-elicited NHP mAbs									Infection bNAbs	
	Strain	Clade	Tier	Q9M-023	Q10M-054	Q10M-055	Q10M-100	Q10M-123	Q12M-032	Q12QBM-007	Q12BBM-023	Q12BBM-069	CH01	PG9
1	Q23_17	A1	1B	0.006	0.025	0.018	0.035	0.030	0.004	0.002	0.001	0.003	0.016	0.014
2	ZM233_6	C	2	0.007	>50	13.1	0.11	0.02	0.009	0.015	0.009	0.009	0.027	0.01
3	CM244_EC1	AE	2	>50	1.02	3.50	2.34	4.23	0.050	0.007	0.007	0.023	0.012	0.016
4	CNE5	01_AE	2	>50	1.24	3.57	8.45	0.38	0.20	0.24	0.15	0.21	0.08	0.02
5	KER018_11	A1	2	>50	0.43	0.59	4.14	1.09	0.10	0.42	0.06	0.35	0.13	0.04
6	DU156_12	C	1B or 2	0.78	1.06	2.05	5.37	1.99	0.72	0.49	0.18	0.20	0.22	0.16
7	3365_V2_C20	A1	2	0.96	1.49	3.84	9.74	4.68	1.77	8.86	0.30	0.68	0.38	0.19
8	246_F3_C10_2	A1C	2	0.73	>50	>50	27.1	3.61	1.84	6.82	0.27	0.96	0.31	0.08
9	BG505.W6M.C2	A	2	0.37	1.58	27.3	21.6	10.8	0.40	0.23	0.05	0.09	0.29	0.09
10	16055_2_3	C	2	0.18	16.7	6.57	1.22	>50	>50	>50	0.09	48.0	7.65	0.05
11	001428_2_42	C	2	0.77	0.53	5.51	2.83	12.1	>50	2.04	0.11	0.15	0.12	0.02
12	ZM249_1	C	2	0.67	3.36	5.96	1.98	1.47	0.65	0.88	0.16	0.44	0.28	0.17
13	25925_2_22	C	1B or 2	0.73	>50	>50	>50	>50	38.0	2.09	0.10	1.00	0.41	0.11
14	BJOX0020	BC	2	0.49	>50	>50	>50	34.2	>50	0.90	0.24	0.42	>50	0.19
15	C1080.c3	01_AE	2	>50	>50	35.7	>50	1.11	>50	1.16	>50	0.01	0.03	0.02
16	CAP45_G3	C	2	>50	0.19	0.54	13.2	>50	>50	>50	>50	0.06	0.04	0.003
17	191955_A11	A1	2	>50	0.14	0.26	4.67	>50	>50	2.27	>50	1.86	0.05	0.04
18	0330_V4_C3	A1	2	2.78	41.2	38.6	>50	>50	>50	27.1	0.15	0.50	0.24	0.04
19	MS208	A1	1 or 2	>50	>50	>50	>50	>50	1.63	1.61	0.25	1.13	27.4	0.25
20	T250-4	02_AG	2	>50	>50	>50	>50	>50	>50	1.51	2.76	0.12	0.06	0.01
21	25710_2_43	C	1B or 2	>50	>50	>50	ND	>50	>50	48.0	2.03	8.99	0.45	0.1
22	92TH021	01_AE	2	>50	>50	>50	>50	>50	>50	2.70	0.46	2.19	0.18	0.2
23	DU422_1	C	2	>50	8.13	16.4	>50	>50	>50	>50	1.64	2.34	31.5	0.56
24	242_14	02A1	1B or 2	>50	>50	>50	>50	>50	>50	3.90	0.13	1.29	0.23	0.09
25	6540_V4_C1	A1C	2	>50	>50	>50	>50	>50	>50	>50	>50	1.76	0.25	0.23
26	Q259_17	A1	2	>50	>50	>50	>50	>50	>50	>50	1.22	3.32	>50	0.25
27	6545_V4_C1	A1C	2	>50	>50	>50	>50	>50	>50	>50	>50	3.90	0.12	0.38
			Median IC_{50}	0.70	1.15	4.68	4.41	1.99	0.53	1.51	0.16	0.50	0.22	0.09

IC_{50} (µg/mL): <0.01 | 0.01 to <0.1 | 0.1 to < 1 | 1 to <10 | 10 to >10

Figure 2

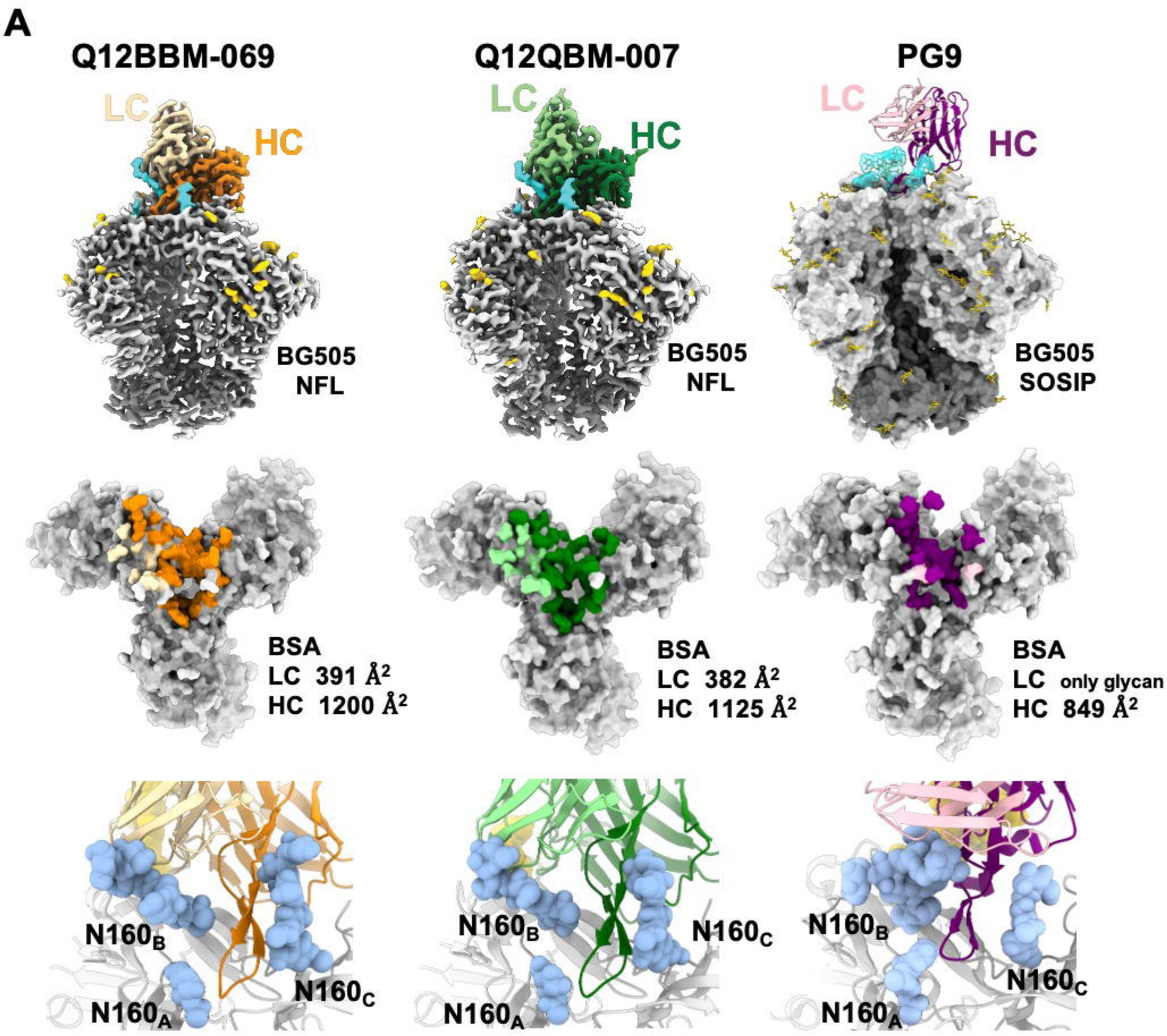

B

mAb	HIV-1 neutralization (IC50, ug/mL) Autologous: Q23.17	Q23.17 N160A	Fold decrease	Heterologous: BG505	BG505 N160A	Fold decrease
Q9M-023	0.006	0.471	79	0.258	>50	>194
Q10M-054	0.025	>50	>2000	4.99	>50	>10
Q10M-055	0.018	>50	>2777	17.1	>50	>2.9
Q10M-100	0.035	0.140	4	23.0	>50	>2.2
Q10M-123	0.030	0.213	7	17.2	>50	>2.9
Q12M-032	0.004	>50	>12500	0.298	>50	>168
Q12QBM-007	0.002	>50	>25000	0.452	>50	>111
Q12BBM-023	0.001	0.095	95	0.071	0.245	3
Q12BBM-069	0.003	0.314	105	0.138	>50	>362
PG9	0.014	>50	>3571	0.112	>50	>446
CH01	0.010	>50	>5000	0.239	>50	>209
RHA1	0.005	0.519	196	0.130	>50	>209

IC_{50} (μg/mL): <0.01 | 0.01 to <0.1 | 0.1 to < 1 | 1 to <10 | 10 to >10

Figure 3

A

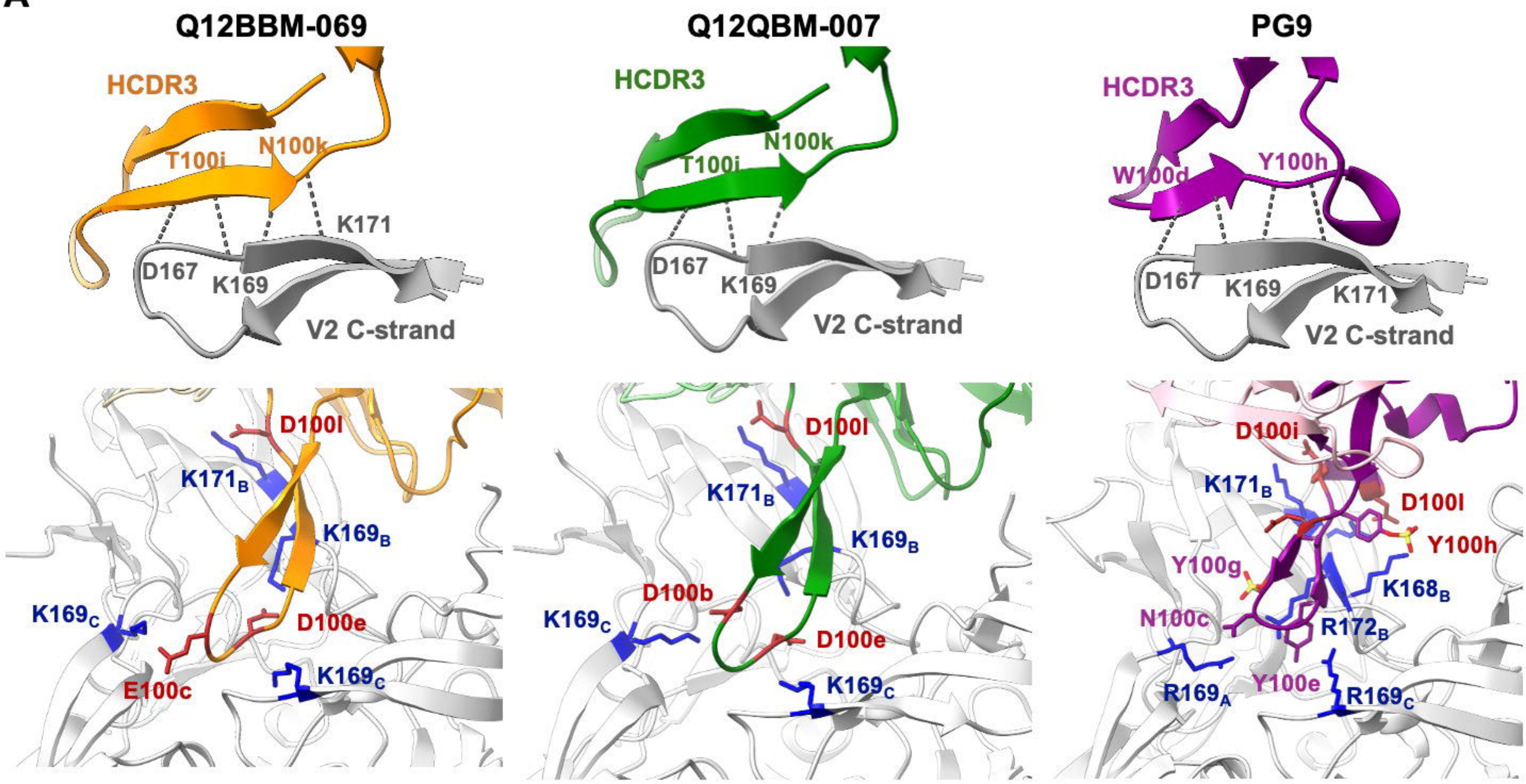

B

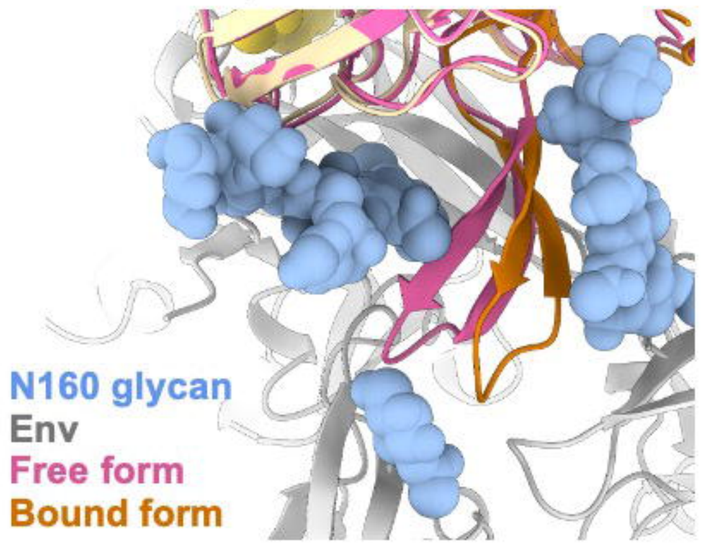

C

	HIV-1 Strain	Neutralization Q12BBM-069	V2 C-strand seq. (164-172)
1	Q23_17		ELRDKRQKV
2	ZM233_6		ELRDKKRKV
3	CM244_EC1		ELRDKKQKV
4	CNE5		ELRDKKQKV
5	KER018_11		ELRDKKRKV
6	DU156_12		ELRDKKQKV
7	3365_V2_C20		EIRDKKQKV
8	246_F3_C10		ELRDKRQKV
9	BG505.W6M		ELRDKKQKV
10	16055_2_3		EIRDKKQKV
11	001428_2_42		EIRDKKQKA
12	ZM249_1		ELRDKKQKV
13	25925_2_22		ELRDKKQKV
14	BJOX0020		ELRDRKQKV
15	C1080.c3		EIRDKKQKV
16	CAP45_G3		ELRDKKQKV
17	191955_A11		EVRDKKQKV
18	0330_V4_C3		ELRDRRQKV
19	MS208		ELRDKKQKV
20	T250-4		ELRDKKKKE
21	25710_2_43		ELRDKKQKV
22	92TH021		EIRDRKQKV
23	DU422_1		ELRDKKQKV
24	242_14		ELRDKKQKV
25	6540_V4_C1		ELRDKKQKV
26	Q259_17		ELRDKKQKV
27	6545_V4_C1		ELRDKRQKV
28	CH070_1	>50	VLRDKKQKV
29	T255_34	>50	ELRDKRRQI
30	R3265_C6	>50	ELKDKKQKI
31	3016_V5_C45	>50	VVRDRKKQV
32	00836_2_5	>50	ELKDKKQSV
33	WITO.33	>50	VIRDKIQKE
34	B41	>50	SIRDKIKKE
35	1056_10_TA1	>50	NIRDKYQKA
36	H080_23	>50	SMQDKIKKN
37	T278_50	>50	LLKDKKKKE
38	CH117_4	>50	ILRDKKKKV
39	16936_2_21	>50	ELRDRKQTV
40	26191_2_48	>50	DVRDKKKTV
41	T252_7	>50	EVSDRKKQE
42	T251_18	>50	ELKDKTKKM
43	92RW020.2	>50	ELKDKKQQV
44	X1632.S2.B10	>50	EIRDKKKQE
45	REJ04541_67	>50	TPRDKIQKE
46	CH119.10	>50	VVRDRQQKV
47	235.47	>50	ELRDKRQNE
48	CNE58	>50	EVRDKKQKK
49	1394C9G1	>50	VVRDKKKKE
50	928_28	>50	ELRDKKKKV
51	X2131_C1_B5	>50	EVRDKQRKE
52	CNE21	>50	EIRDKKHKE

IC50 (μg/mL): <0.01 | 0.01 to <0.1 | 0.1 to < 1 | 1 to <10 | 10 to >10

D

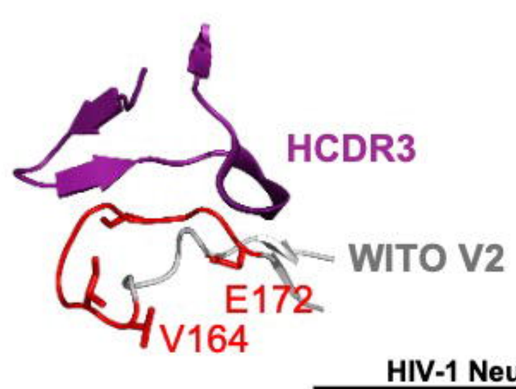

	WITO4160.33 C-strand 164-172	HIV-1 Neutralization IC50 Total IgG P6 Q7	Total IgG P6 Q8	mAbs PG9	mAbs VRC26	
WT	VIRDKIQKE	1930	455	0.41	>50	
I169R	VIRDKRQKE	261	4.8	0.27	15.7	KI
K168E	VIRDEIQKE	>2000	>2000	>50	>50	KO
I169E K171E	VIRDKEQEE	>2000	>2000	>50	>50	KO
Q23.17	ELRDKRQKV					

Figure 4

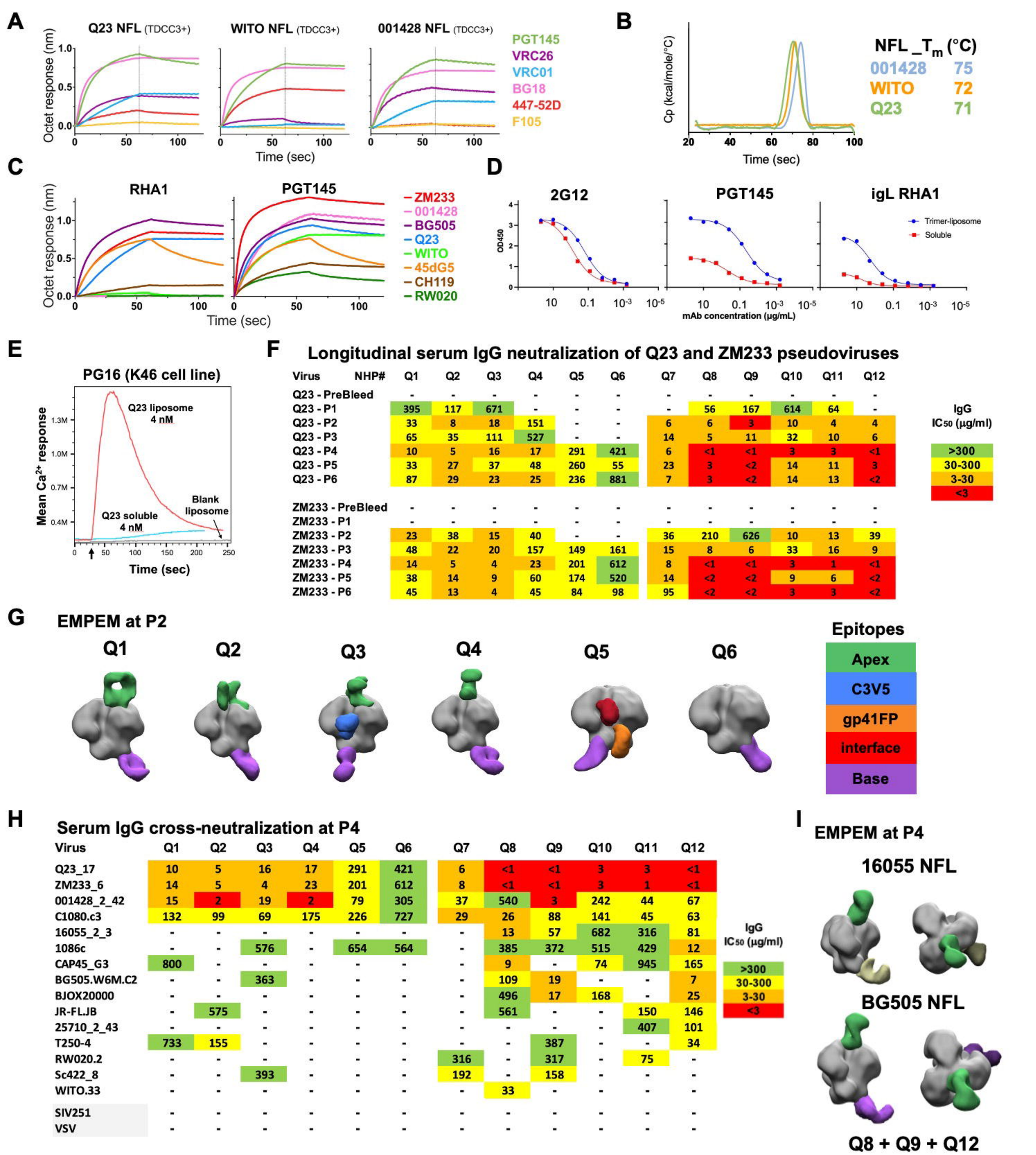

Figure S1. Biochemical analysis of NFL trimers, trimer-liposomes, serum and EMPEM analysis, related to Figure 1. (A) BLI binding of NFL trimers to representative antibodies. **(B)** DSC of NFL trimers **(C)** BLI binding of RHA1 and PGT145 to NFL trimers. **(D)** ELISA binding data of Q23 NFL trimer-liposomes. **(E)** Calcium flux analysis against PG16 cells. **(F)** Longitudinal neutralization titers (IC_{50}) against Q23.17 and ZM233.6 pseudoviruses. **(G)** EMPEM analysis of Q1-Q6 NHPs at P2. **(H)** Neutralization titers against a panel of clinical isolates at P4. **(I)** EMPEM analysis of pooled serum at P4 reveals cross binding density at trimer-apex (green) against two different Env trimers not from the immunogen series.

A

NHP ID	mAb ID	lineage name	Q23_17	ZM233_6	001428_2	16055_2_3	BG505.W6M	CAP45_G3	C1080.c3	DU156_12	BJOX0020	25710_2_43	SIV251
			HIV-1 neutralization (IC_{50}, µg/mL)										
Q9	Q9M-023	Q9M-023	<0.05	<0.05	0.77	0.18	0.37	>50	>50	0.78	0.49	>50	>50
	Q9M-009		<0.05	<0.05	>50	>50	>50	>50	>50	>50	>50	>50	>50
	Q9M-092		0.09	0.12	0.61	4.36	>50	>50	>50	2.33	1.05	>50	>50
	Q9M-001		0.21	<0.05	>50	>50	>50	>50	>50	>50	1.57	>50	>50
Q10	Q10M-055	Q10M-055	<0.05	13.14	5.51	6.57	27.26	0.54	35.69	2.05	>50	>50	>50
	Q10M-054		<0.05	>50	0.53	16.70	1.58	0.19	>50	1.06		>50	>50
	Q10M-061		<0.05	0.16	11.50	>50	>50	>50	>50	2.86		>50	>50
	Q10M-092		<0.05	<0.05	>50	>50	>50	>50	>50	5.05		>50	>50
	Q10M-113		0.12	>50	>50	>50	>50	>50	>50	27.25	>50	>50	>50
	Q10M-100	Q10M-100	<0.05	0.13	2.83	1.22	21.55	13.22	>50	5.37	>50		>50
	Q10M-123		<0.05	<0.05	12.07	>50	10.79	>50	1.11	1.99		>50	>50
	Q10M-048	Q10M-048	3.12	0.28	>50	>50	>50	>50	>50	>50	>50		>50
	Q10M-103		>50	>50	>50	>50	>50	>50	>50	>50	>50		>50
	Q10M-083		0.40	<0.05	>50	>50	>50	>50	>50	>50		>50	>50
	Q10M-112		>50	8.08	>50	>50	>50	>50	>50	>50		34.00	>50
	Q10M-122		>50	3.04	>50	>50	>50	>50	>50	>50		>50	>50
	Q10M-137		>50	4.51	>50	>50	>50	>50	>50	>50		>50	>50
	Q10M-209		>50	>50	>50	>50	>50	>50					>50
Q12	Q12BBM-069	Q12BBM-069	<0.05	<0.05	0.15	48.00	0.09	<0.05	<0.05	0.20		8.99	>50
	Q12M-165		<0.05	<0.05	0.42	1.23	0.21	>50	>50	0.29	1.16	23.70	>50
	Q12M-061		<0.05	<0.05	1.35	>50	0.89	>50	0.63	1.24	>50	>50	>50
	Q12QBM-007	Q12QBM-007	<0.05	<0.05	2.04	>50	0.23	>50	1.16	0.49	0.9	48	>50
	Q12BBM-023		<0.05	<0.05	0.11	0.09	0.05	>50	>50	0.18		2.03	>50
	Q12BBM-068		<0.05	<0.05	0.25	0.09	0.05	>50	>50	0.23		4.11	>50
	Q12M-031		<0.05	<0.05	>50	>50	0.19	>50	>50	1.5	>50		>50
	Q12M-032	Q12M-131	<0.05	<0.05	>50	>50	0.4	>50	>50	0.72	>50	>50	>50
	Q12M-035		0.83	<0.05	>50	>50	>50	>50	>50	>50	>50	>50	>50
	Q12M-131		>50	<0.05	>50	>50	>50	>50					>50
	Q12M-158		>50	<0.05	>50	>50	>50	>50					>50
	Q12M-197		>50	<0.05	>50	>50	>50	>50					>50
	Q12M-190	Q12M-190	0.27	>50	>50	>50	>50	>50					>50
	Q12M-283		>50	>50	>50	>50	>50	>50					>50
	Q12BBM-045	Q12BBM-045	>50	0.8	>50	>50	>50	>50	>50	>50	>50	>50	>50
	Q12QBM-034		>50	0.19	>50	>50	>50	>50	>50	>50	>50	>50	>50
	Q12BBM-056		>50		>50		>50	>50		>50	>50		>50
	Q12BBM-065		>50		>50		>50	>50		>50	>50		>50
	Q12BBM-085		>50		>50		>50	>50		>50	>50		>50
	Q1216M-031	Q1216M-031	>50	>50	>50	>50	>50	>50					>50
	Q12B16M-007		>50	>50	>50	>50	>50	>50					>50
	Q12BBM-042	Q12BBM-042	>50		>50		>50	>50		>50	>50		>50
	Q12BBM-076		>50	>50	>50	>50	>50	>50	>50	>50	>50	>50	>50
	Q12BBM-022	Q12BBM-022	>50	>50	>50	>50	>50	>50	>50	>50	>50	>50	>50
	Q12BBM-026		>50		>50		>50	>50		>50	>50		>50
	Q12BBM-044		>50		>50		>50	>50		>50	>50		>50
	Q12BBM-043		>50		>50		>50	>50		>50	>50		>50

IC_{50} (µg/mL): <0.1 | 0.1 to < 1 | 1 to <10 | 10 to >10

B

	Strain	CLADE	TIER	Vaccine-elicited NHP mAbs: Q9M-023	Q10M-054	Q10M-055	Q10M-100	Q10M-123	Q12M-023	Q12QBM-007	Q12BBM-023	Q12BBM-069	human bNAbs: RHA1	PG9
28	CH070_1	07_BC	3	>50	>50	>50	>50	>50	>50	>50	>50	>50	0.09	0.02
29	T255_34	02_AG	2	>50	>50	>50	>50	>50	>50	>50	>50	>50	0.07	0.07
30	R3265_C6	AE	2	>50	>50	>50	>50	>50	>50	>50	>50	>50	>50	0.37
31	3016_V5_C45	D	2	>50	>50	>50	>50	>50	>50	>50	>50	>50	0.22	0.32
32	00836_2_5	C	1B or 2	>50	>50	>50	31.6	>50	>50	>50	>50	>50	>50	>50
33	WITO.33	B	2	>50	>50	ND	>50	>50	ND	>50	>50	>50	0.03	0.04
34	B41	B	2	>50	>50	>50	>50	>50	>50	>50	>50	>50	0.63	0.13
35	1056_10_TA11	B	1B or 2	>50	>50	>50	>50	>50	>50	>50	>50	>50	>50	>50
36	H080_23	B	2	>50	>50	>50	>50	>50	>50	>50	>50	>50	>50	0.36
37	T278_50	02_AG	2 or 3	>50	>50	>50	>50	>50	>50	>50	>50	>50	5.42	0.97
38	CH117_4	07_BC	2	>50	>50	>50	>50	>50	>50	>50	>50	>50	0.14	0.03
39	16936_2_21	C	2	>50	>50	>50	>50	>50	>50	>50	>50	>50	>50	>50
40	26191_2_48	C	2	>50	>50	>50	>50	>50	>50	>50	>50	>50	0.21	0.34
41	T252_7	A1G	2	>50	>50	>50	>50	>50	>50	>50	>50	>50	>50	0.19
42	T251_18	02_AG	2 or 3	>50	>50	>50	>50	>50	>50	>50	>50	>50	>50	>50
43	92RW020.2	A1	2	ND	>50	>50	>50	>50	>50	>50	>50	>50	14.72	0.36
44	X1632.S2.B10	G	2	ND	>50	>50	>50	>50	>50	>50	>50	>50	0.25	0.25
45	REJ04541_67	B	2	ND	>50	ND	ND	ND	ND	>50	>50	>50	0.26	0.03
46	CH119.10	BC	2	ND	>50	ND	ND	ND	>50	>50	>50	>50	32.14	1.64
47	235.47	AG	2	>50	>50	>50	>50	>50	>50	>50	>50	>50	0.19	0.24
48	CNE58	C	1B or 2	>50	>50	>50	>50	>50	>50	>50	>50	>50	0.13	0.07
49	1394C9G1	C	2	>50	>50	>50	>50	>50	>50	>50	>50	>50	0.09	0.08
50	928_28	02_AG	2	>50	>50	>50	>50	>50	>50	>50	>50	>50	>50	0.2
51	X2131_C1_B5	G	2	>50	>50	>50	>50	>50	>50	>50	>50	>50	4.06	0.32
52	CNE21	BC	1B	>50	>50	>50	>50	>50	>50	>50	>50	>50	0.25	0.15
+ N130 glycan viruses														
53	CH505.TF	C	2	>50	>50	>50	>50	>50	>50	24.1	36.1	42.1	0.05	0.32
54	Q168.a2	AD	2	ND	>50	>50	>50	>50	>50	>50	>50	>50	ND	ND
55	PVO.04	B	2 or 3	ND	>50	>50	ND	>50	>50	>50	>50	>50	>50	>50
56	ZM197.7	C	1B	ND	>50	>50	>50	>50	>50	>50	>50	>50	ND	ND
57	TRO.11	B	2	ND	>50	ND	ND	ND	>50	>50	>50	>50	>50	>50
58	Ce1086_B2	C	2	>50	>50	>50	>50	>50	>50	>50	>50	>50	>50	>50
59	94UG103	A1	2	>50	>50	>50	>50	>50	>50	>50	>50	>50	2.86	1.46
60	C4118	AE	2	>50	>50	>50	>50	>50	>50	>50	>50	>50	0.32	0.15
61	CAP256_SU	C	2	>50	>50	>50	>50	>50	>50	>50	>50	>50	0.25	0.06
62	SC422_8	B	2	ND	>50	>50	ND	>50	>50	>50	>50	>50	ND	0.64
63	191859	D	2	>50	>50	>50	>50	>50	>50	>50	>50	>50	>50	>50

IC_{50} (µg/mL): <0.1 | 0.1 to < 1 | 1 to <10 | 10 to >10

Figure S2. Neutralization titers of mAbs, related to Figures 1 and 2. (A) Initial screening of 45 mAbs cloned from Q9, Q10 and Q12 NHPs against a small panel of viruses to select mAbs with cross-neutralizing activity. **(B)** Cross-neutralizing mAbs against additional viruses lacking N130 glycan (light brown) and viruses with N130 glycan (dark brown).

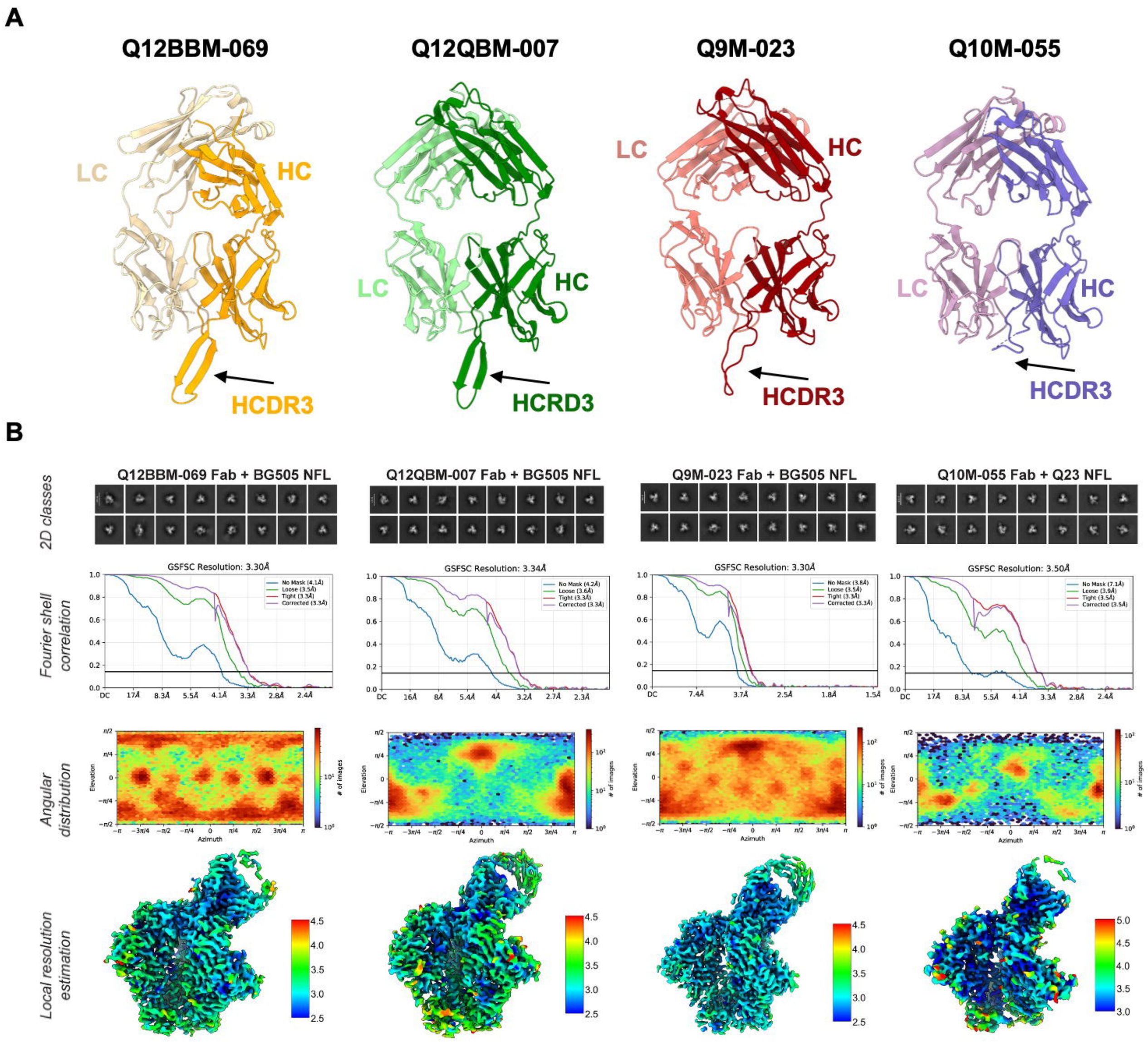

Figure S3. Crystal structures of Fabs and CryoEM reconstruction statistics, related to Figures 3 and 4. (A). Crystal structures of unliganded Fabs. HCDR3 is labeled. **(B)** Representative 2D class averages, Fourier shell correlation resolution estimate, angular distribution of observations, and local resolution estimation (in Å) of the cryo-EM datasets.

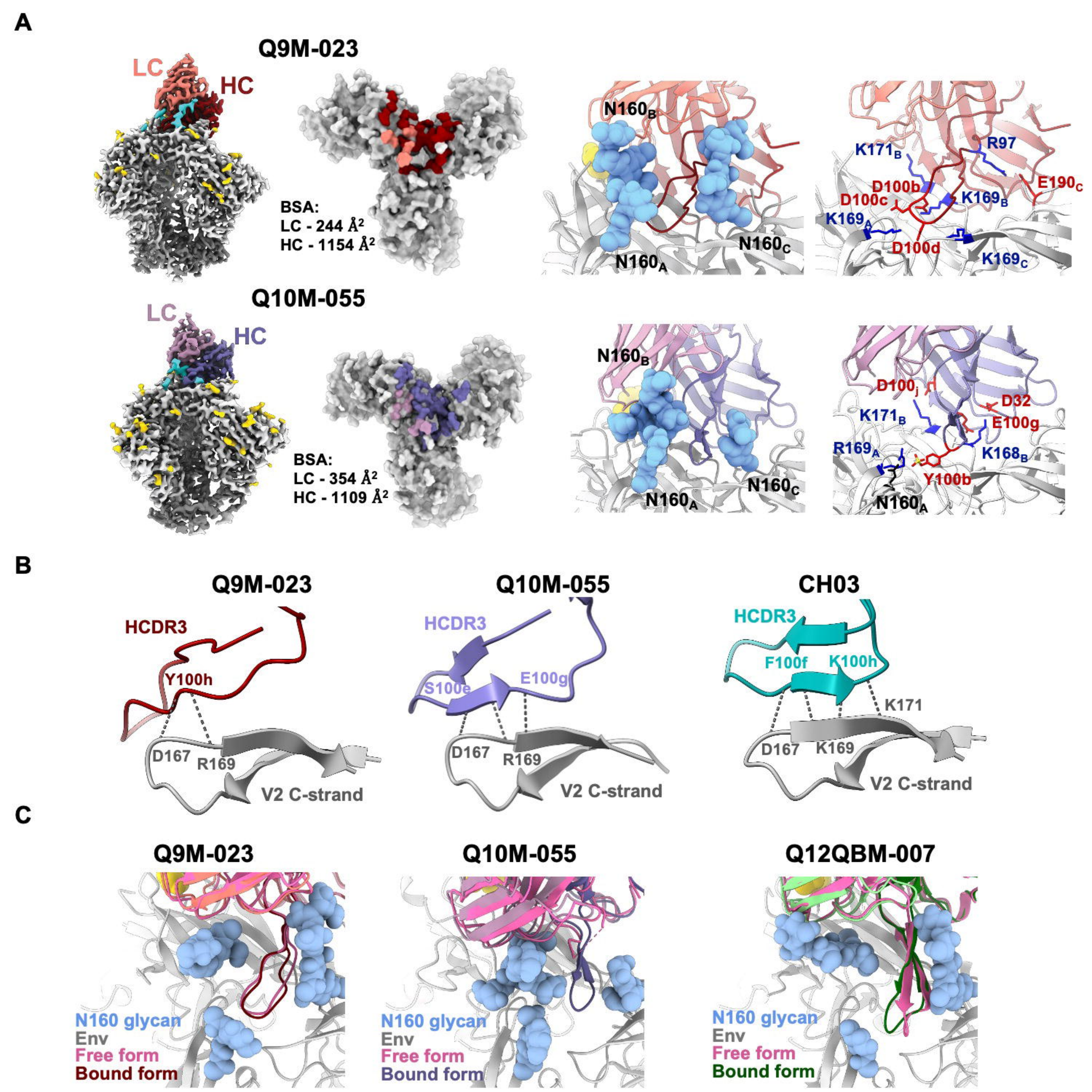

Figure S4. CryoEM complex structures of Q9M-023 and Q10M-055, interaction with V2 C-strand, comparison to the unliganded HCDR3, related to Figures 3 and 4. (A) CryoEM maps, epitope footprint, HCDR3 interactions with N160 glycan, and key contact residues of Q9M-023 in complex with BG505 NFL (top row) and Q10M-055 with Q23 NFL. Glycans at N160 position are colored blue, all other glycans are colored yellow. **(B)** Interaction of HCDR3 with C-strand, compared to bNAb CH03. Hydrogen bond interactions are shown as dotted lines. **(C)** Superposition of HCDR3 loops from (unliganded) crystal structures to cryoEM complex structures.